R E Z U M A T

TEZĂ DE DOCTORAT

CERCETĂRI TEORETICE ŞI EXPERIMENTALE PRIVIND SOLICITĂRILE DEZVOLTATE ÎN SISTEMELE UZUALE FOLOSITE PENTRU ANCORAREA ECHIPAMENTELOR TEHNOLOGICE AGABARITICE TRANSPORTATE

THEORETICAL AND EXPERIMENTAL RESEARCH REGARDING THE STRESSES DEVELOPED IN SYSTEMS COMMONLY USED FOR ANCHORING TRANSPORTED OVERSIZED TECHNOLOGICAL EQUIPMENT

Autor: ing. STĂTESCU MIHAI

Conducător de doctorat:
Prof. univ. emerit dr. ing. IATAN I. RADU

BUCUREŞTI
2020

FOREWORD

"Research means that you do not know, but want to know."
Charles F. Kettering

This research is the result of my desire to discover and also to provide colleagues with a basis, a collection of information to refer to when they are put in the position to provide life-saving solutions for anchoring oversized technological equipment, during their transportation. This PhD thesis crowns all my work during my engineering career and opens my appetite for research and continuous development. The preparation of the thesis meant for me not only a lot of effort and concern, but also enormous satisfactions, which I feel that this paper crowns.

In order to elaborate this PhD Thesis, I was coordinated and guided with great exigency by **Mr. Prof. univ. emeritus Dr. Eng. Radu I. Iatan**, whom I thank for his support, his spirit of his scientific intransigence, high professionalism and outstanding pedagogical qualities.

Considering that the applications specific to the experimental research took place in the laboratories of the Department of Materials Strength, of the Faculty of Mechanical and Electrical Engineering, within the University of Petroleum - Gas from Ploiești, I would like to address special thanks and distinguished consideration to **Mr. Prof. univ. dr. eng. Șerban VASILESCU** for the support provided in performing the experimental analyzes, as well as for the kindness to be part of the Thesis Evaluation Commission, together with Mr. Dean - **Prof. univ. dr. eng. Cristian PAVEL** of the Faculty of Technological Equipment for Constructions within UTCB, to whom I thank very much for the availability and goodwill shown for this purpose.

I also want to address my feelings of warm thanks and gratitude to the teachers from the Doctoral Guidance Commission within the Department of Equipment for Industrial Processes, respectively to **Prof. univ. dr. eng. Teodor SIMA**, **Mr. Lecturer dr. eng. Ion Durbacă**, and **Ms. Lecturer dr. eng. Georgiana Luminița Enăchescu**, as well as the entire team of teachers from the Department.

On this occasion, I feel obliged to thank the secretariat of the Doctoral School of the Faculty of Mechanical and Mechatronics Engineering for their kindness, goodwill and understanding given throughout the doctoral preparation.

I would also like to thank Engineer Mircea Oprea, manager at ASSET Oltenia, IREM SPA, for the help provided in order to achieve the experimental model.

Doresc sa adresez mulțumiri și Domnului Inginer Mircea Oprea, manager la ASSET Oltenia, IREM SPA, pentru ajutorul acordat în vederea realizării modelului experimental.

I can't help but remember the remarkable contribution of my family, to whom I thank and will always be grateful for the understanding, encouragement and support provided throughout the period of doctoral preparation and thesis development.

<u>Note</u>: The bibliographic sources indicated below are set out at the end of each chapter of the Doctoral Thesis.

CHAPTER 1

BRIEF HISTORY REGARDING THE TRANSPORTATION OF OVERSIZED AND / OR HEAVY TECHNOLOGICAL EQUIPMENT

1. 1. INTRODUCTION

Transportation of industrial products, appeared as a distinct branch, at the end of the 15th century, having consistency with the industrial revolution. Until the beginning of the 19th century, the transport was made only by land and by water. In the beginning, domestic animals were used to move different weights.

The transport of industrial equipment to the construction site can be done by rail, road, water (river or sea, by barge or directly by flotation) and by air. The transport of the structures inside the construction sites is done on access railways, on roads arranged provisionally or definitively. In most cases, the transportation of oversized technological equipment is done by combining several such methods.

Rail, car, sea, air transport is an important field of the economic and social activity, through which the movement or relocation of goods and people is carried out, in order to satisfy the material and spiritual interests of human society..

1. 1. 2. Road transport

In terms of costs, the duration required for the transport operation, the technical condition of the bridges and roads along the route, as well as the dependence on the weather, road transport is clearly disadvantageous compared to rail. There are some characteristic **disadvantages [10 - 12]:**

a) road transport for oversized and heavy equipment, is not performed in bad weather: fog, torrential rain, frost, heavy snow, strong wind, etc.;

b) during the movement of such transports, the power supply, of electric and telephone lines may be interrupted..;

c) the road transport project involves a detailed study of the route, of the permissible masses and sizes and even measurements in places where the dimensions of the cargo-vehicle assembly are close to those of the so-called narrow areas.

In the case of road transport, some **advantages** should be noted, among which **[11 - 13] :**

a) rapid adaptation of operations to any field conditions;

b) the production of vehicles for transport has lower specific investments, and the training of the drivers of such operations requires lower costs compared to other types of transport.;

c) diesel traction is much more economical than the gasoline-based one;

d) equipment is loaded directly from the place of shipment / manufacturer;

e) smaller areas required to achive the traffic routes;

f) lower global investment.

When finalizing the choice of the road transport solution, the cost of assembly and installation on site, as well as the cost of the necessary loading and unloading operations must be included. Once they have been established, it is important to obtain the necessary approvals from the law enforcement bodies, in each case. **[15]**

In some cases, in addition to these approvals, the following may be required:

- Carrying out additional road diversion works;
- Widening of certain sections of roads;
- Making embankments;
- Consolidation of roads and bridges, etc.

In order to safely transport the equipment and protect their integrity, these possible additional arrangements must be taken into account..

The vehicle traveling in excess of the minimum permissible masses and / or dimensions must be additionally accompanied by a traffic police crew, for:

- Width greater than 5,0 m;
- Length greater than 40,0 m;
- Height greater than 5,0 m;
- Total mass greater than 80,0 tons.

Fig. 1. 4. Oversized transport convoy **[21]**

Fig. 1. 6. Transport with a length of 110 m **[22]**

A particularly important condition is the training of personnel in the safety technique for lifting and the use of adequate protective equipment.

Some examples of transporting oversized technological equipment by road are illustrated in the figures 1. 4, 1. 6.

1. 1. 3. Rail transport

The beginning of rail transport is due to the invention of the steam locomotive by ***George Stephenson*** in 1815, the first railway in the world being inaugurated on September 15, 1830 in England. This connected the cities of Liverpool and Manchester. **[5].**

Rail transport, unlike other types of transport, has a number of **advantages [15]:**

a) very low costs for the actual transport operation;

b) it does not require investments for the construction of roads or the purchase of means for transportation and eventual handling;

c) the transport can be carried out at any time of the year, without depending, practically, on the meteorological conditions;

d) the duration of the transport is reduced;

e) it does not require blocking of the roads, the interruption of the power supply, of the telephone lines etc.;

f) requires fewer formalities for obtaining free movement permits compared to other types of transport.

Some specific examples of transporting oversized equipment by rail are shown in the figures 1. 9 – 1. 10.

Fig. 1. 9. Oversized transport by train **[17]**

Fig. 1. 10. Oversized transport by train **[18]**

1. 1. 4. Transportation by water

Also this type of transport has known its own evolution and history. Technical innovations have been an essential element in the development of navigation. The use of steel, instead of wood, in the construction of ships had a significant effect, with a special influence on the load capacity. In the same sense, it was necessary to use the steam engine, and later the explosion engine, increasing the travel speed.

Transport on water is recommended especially for very long distances, being almost free of size and tonnage problems. In this situation, the transport of the equipment can be done on self-propelled or towed ships.

The movement of the ship translates into loads on the two main axes of the vessel. Transport brackets and fastening cables must be strong enough to withstand the effect of external forces. The point of application of these loads is in the center of gravity of the equipment, they stress the structure in the same way as the seismic forces.

Fig. 1. 12. Equipment stored on deck **[26].**

Fig. 1. 13. Equipment stored under the deck **[26].**

The main concern of the design engineer is to translate the loads resulting from the movement of the ship into loads that apply to the equipment, it being stored either on deck (fig. 1. 12) or under the deck (fig. 1. 13).

Fig. 1. 14. Ship with the possibility of immersion **[27].** **Fig. 1. 15.** Barge transport on the Danube **[28]**

There are also ships with immersion possibilities (fig. 1. 14).

Submersible ships are also known as float-on and float-off. In appearance, these ships are similar to bulk carriers (ships specializing in the transport of solid goods in bulk).

Barges are another means of transporting oversized technological equipment by water. The barge is usually used as an intermediate means of transport by waterways such as rivers, to reach the ocean or sea with the cargo.

1. 1. 5. Transportation by air

Fig. 1. 16. Loading on an Antonov plane AN-225 **[29].**

Such transports are used in special cases, when the installation of equipment is carried out in isolated places (in mountains, in wooded places, without access roads). The means used for transportation are high-capacity helicopters and airships.

Air transportation is done with means that have **advantages**:

a) does not require traffic routes;

b) they have high speeds;

c) they can be easily routed to different points where transportation is needed.

Disadvantages include: high fuel consumption, relatively low load capacity, high transportation costs, the need to use expensive construction materials and a high degree of technicality. **[24]**.

A correct choice of transport possibilities will be made only by analysis on variants, taking into account both the advantages and the specific disadvantages.

Nowadays, many aircraft conversions are performed, especially older ones, which are no longer suitable for travel, often due to changing safety or noise requirements, or when the aircraft type is considered to have become uncompetitive in the aitline service for passenger travel.

The main advantage of aircraft specific to oversized transport is that they have been specially designed to serve such services and provide special loading / unloading methods, floors and special configuration.

1. 1. 6. General remarks

One of the main concerns of designers and manufacturers of oversized technological equipment is to identify the difficulties that may arise during the ytansportation of these structures, from manufacturer to beneficiary.

The emergence and development of oversized transport, as it is known, can be observed since 1970. This could happen considering the technical / technological progress that allowed the construction and production of ever larger industrial objects. Another important factor that led to the development of oversized transport was the oil crisis. This has led Northern European countries to start extracting crude oil on their own in order to get a better price. In less than a year, massive oversized shipments were made to the North Sea to start oil exploration operations.

Recently, in addition to the special attention paid to the design of technological equipment, importance has also begun to be given to transportation operations. When these transported constructions exceed the sizes (specific to roads or railways) that allow the movement in one piece, the subassemblies, processed in specialized enterprises, are brought to the site. This transport process is usually chosen in the case of metal constructions that are manufactured in enterprises or in specially arranged workshops.

The current trend is to deliver completely assembled industrial constructions to the beneficiary, thus reducing the handling time, assembly and, obviously, the related costs.

1. 2. Research directions for the thesis

Taking into account the characteristics of oversized transports, specified above, for the realization of the content of the thesis, the following general aspects are taken into account:

a) Literature study on the evaluation of the forces necessary to tow, in a straight line or in a curve, an oversized convoy with large mass, conditioned by the characteristics of the route (in the present case a flat surface without unevenness), the loads developed by the actual load (static and / or inertial), the meteorological conditions that can change the state of the road, as well as the wind effect.

b) Literature study on the stability of the longitudinal movement of towing devices or convoys (means for tractors - platforms loaded with oversized equipment), depending on external loads (mass forces, inertia forces, as well as wind action and road conditions).

c) Transverse stability of the movement of loaded platforms under conditions similar to those in point b).

d) Literature study on the calculation of sizing or checking of welded flat lugs and trunnions for lifting or anchoring oversized and high-mass technological equipment.

e) Own theoretical and experimental studies regarding constructions of cylindrical trunnions and lugs for anchoring / lifting loads.

f) Conclusions, contributions and perspectives.

CHAPTER 2

CALCULATION ELEMENTS OF TOWING FORCES OF PLATFORMS LOADED WITH OVERSIZED INDUSTRIAL EQUIPMENT

2. 1. Introduction

The final technological / functional safety of mechanical equipment is guaranteed by the quality of all the stages from conception to commissioning and operation. Of all these stages, the transport of oversized industrial technological equipment, from the manufacturer to the user, stands out with its significant economic importance **[6, 7].**

Placing such equipment on the transport platforms, anchoring them securely (in difficult weather conditions, from a meteorological and / or wind point of view, usually difficult to predict), as well as unloading at the site (construction sites) on foundations involves the use of appropriate construction systems, with well-defined bearing capacity **[6].** The global analysis of an oversized transport considers not only the legal and constructive and human safety aspects, but also the economic, social and environmental ones **[8 – 15, 35, 44, 47 - 50].**

In order to achieve the most rational transports (technical and economic) satisfying the desired requirements, these companies have introduced in the design of trailers and semi-trailers (used as platforms for loading and transporting equipment) the term "**modular**". In this sense it is possible to combine several elements for transport called "**modules**" and standard attachments, compatible for the transported equipment **[16].**

Trailers can be made up with 2 to 10 line transport modules, coupled longitudinally or transversely **[6, 16, 30].** Among their **advantages** are recorded:

a) the construction that allows the necessary commands to be performed remotely;

b) lightweight structure; compared to the mass of the load is up to 20 times smaller;

c) possibility to adapt easily, taking into account the mass, shape, driving conditions, permissible axle or wheel load, road slope etc.;

d) taking into account the mass, shape, driving conditions, permissible axle or wheel load, road slope, etc., an easy change is possible;

e) short duration of making combinations in width and length;

f) quick connection of elastic, hydraulic and pneumatic systems between modules;

g) quick assembly and disassembly of the end corssmember.

Among the ***advantages of semi-trailers*** are mentioned **[6, 16]:**

a) superior maneuverability;

b) easy inscription in curves with smaller medium radii;

c) the possibility of easier and safer coupling with the tractor;

d) reversing easier;

e) the possibility of transporting long and bulky loads, due to a larger area of use of the platform;

f) reducing the length of the road train (convoy);

g) an improvement in road safety is achieved, for higher travel speeds due to better connections between towing mechanisms.

There are also some ***disadvantages***:

a) the oscillations of the tractor, especially those in relation to the transverse axis are unpleasant for driving, due to the short wheelbase of the tractor with saddle;

b) when climbing ramps, due to the uneven distribution of the mass / weight of the transported equipment - platform on the rear axles, the adhesion is reduced.

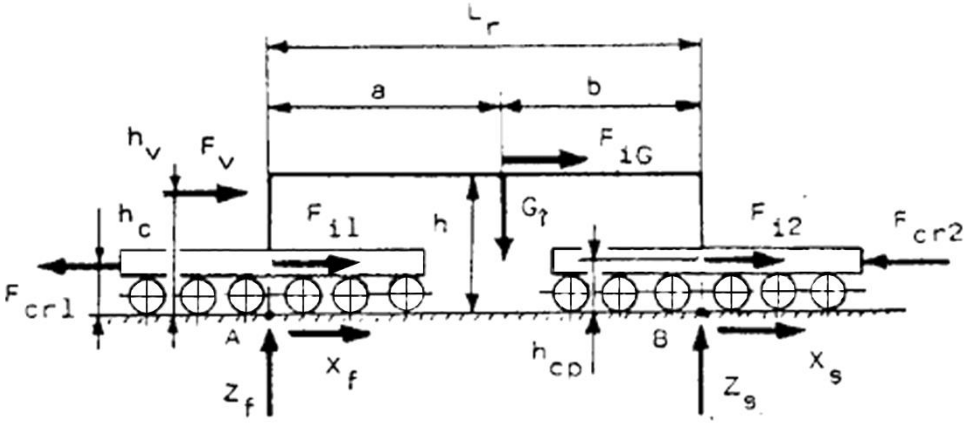

Fig. 2. 1. Transport system with two distant trailers (sketch) **[6, 29]**

The general cost of the transport operation must also include the possibility of carrying out additional works to divert existing roads, widening sections of roads, building embankments, consolidating roads and bridges, etc..**[6, 31, 34].** Finally, after establishing the mode of transport, it is important to obtain, from the official bodies of law, the necessary approvals for each case. **[8, 9].**

Among the performances of towing vehicles, the most important are: maximum speed, acceleration capacity at start (duration and starting space, acceleration, average speed), the ability to climb or descend slopes, braking capacity **[20, 27].** In the category of vehicles used to form ***road trains*** (combinations of towing means, semi-trailers and trailers) includes **cars** (trucks and saddle tractors) with wheeled tread and tractors with wheeled, crawler or semi-tracked tread **[18, 43].** Elements regarding the evaluation of vehicle forces are presented in the paper **[6,** p. 136 - 145**],** for example:

2. 2. Systems with two distant modules [29]

2. 2.1. Moving in a straight line

Case 1. It is considered that the movement of the convoy is done in a straight line, in ***acceleration mode, on a horizontal road, without unevenness*** **[6, 29].** It is used for towing distant trailers, two tractors, placed in front and behind the assembly (simulated by the presence of forces on the hooks F_{cr1} şi F_{cr2} - fig. 2. 1).

Note: It is assumed that all platform axles are evenly loaded.

After writing the balance of bending moments in relation to points *A* and *B* (fig. 2. 1), the expressions of the reactions result **[6]:**

$$Z_f = \frac{G_{\hat{i}} \cdot b + G_{pf} \cdot L_r - F_{iG} \cdot h - \left(F_{i1} + F_{i2}\right) \cdot h_{cp} + \left(F_{cr1} + F_{cr2}\right) \cdot h_c - F_v \cdot h_v}{L_r}; \quad (2.\ 1)$$

$$Z_s = \frac{G_{\hat{i}} \cdot a + G_{ps} \cdot L_r + F_{iG} \cdot h + \left(F_{i1} + F_{i2}\right) \cdot h_{cp} - \left(F_{cr1} + F_{cr2}\right) \cdot h_c + F_v \cdot h_v}{L_r}, \quad (2.\ 2)$$

Case 2. This time the transport convoy moves in a straight line, in ***braking mode, on a horizontal road, without unevenness*** **[6, 29]** The vehicle positioned in front of the convoy moves in towing mode, and the one placed behind the convoy works in braking mode (in the calculations performed, the direction of the inertial forces and the sign of the force F_{cr2} change - fig. 2. 1). In the above conditions, based on the equations of equilibrium of the bending moments with respect to points *A* and *B* (fig. 2. 1), the equalities are deduced **[6]:**

$$Z_f = \frac{G_{\hat{i}} \cdot b + G_{pf} \cdot L_r + F_{iG} \cdot h + \left(F_{i1} + F_{i2}\right) \cdot h_{cp} + \left(F_{cr1} - F_{cr2}\right) \cdot h_c - F_v \cdot h_v}{L_r}; \quad (2.\ 5)$$

$$Z_s = \frac{G_{\hat{i}} \cdot a + G_{ps} \cdot L_r - F_{iG} \cdot h - \left(F_{i1} + F_{i2}\right) \cdot h_{cp} - \left(F_{cr1} - F_{cr2}\right) \cdot h_c + F_v \cdot h_v}{L_r}, \quad (2.\ 6)$$

Case 3. The transport system moves in a straight line, ***uniformly accelerated, on a sloping road at an angle*** α_l, ***without unevenness*** **[6, 29].** The expressions of the reactions with respect to points *A* and *B* (fig. 2. 1) appear in the forms **[6]:**

$$\begin{aligned} Z_f = \Big[& G_{\hat{i}} \cdot \left(b \cdot \cos\alpha_l - h \cdot \sin\alpha_l\right) + G_{pf} \cdot \left(L_r \cdot \cos\alpha_l - h_{cp} \cdot \sin\alpha_l\right) - \\ & - F_{iG} \cdot h - \left(F_{i1} + F_{i2}\right) \cdot h_{cp} + \left(F_{cr1} + F_{cr2}\right) \cdot h_c - F_v \cdot h_v \Big] \Big/ L_r; \end{aligned} \quad (2.\ 9)$$

$$\begin{aligned} Z_s = \Big[& G_{\hat{i}} \cdot \left(a \cdot \cos\alpha_l + h \cdot \sin\alpha_l\right) + F_{iG} \cdot h + G_{ps} \cdot \left(L_r \cdot \cos\alpha_l - h_{cp} \cdot \sin\alpha_l\right) + \\ & + F_{iG} \cdot h + \left(F_{i1} + F_{i2}\right) \cdot h_{cp} - \left(F_{cr1} + F_{cr2}\right) \cdot h_c + F_v \cdot h_v \Big] \Big/ L_r, \end{aligned} \quad (2.\ 10)$$

Case 4. In case of moving the convoy ***on a sloping road at an angle*** α_l, ***without bumps, in uniform braking mode on a slope*** **[6, 29],** the reactions have the following formulas:

$$\begin{aligned} Z_f = \Big[& G_{\hat{i}} \cdot \left(b \cdot \cos\alpha_l + h \cdot \sin\alpha_l\right) + G_{pf} \cdot \left(L_r \cdot \cos\alpha_l - h_{cp} \cdot \sin\alpha_l\right) - \\ & - F_{iG} \cdot h + \left(F_{cr1} - F_{cr2}\right) \cdot h_c - F_v \cdot h_v \Big] \Big/ L_r; \end{aligned} \quad (2.\ 12)$$

$$\begin{aligned} Z_s = \Big[& G_{\hat{i}} \left(a \cdot \cos\alpha_l - h \cdot \sin\alpha_l\right) + F_{iG} \cdot h + G_{ps} \cdot \left(L_r \cdot \cos\alpha_l - h_{cp} \cdot \sin\alpha_l\right) - \\ & - \left(F_{cr1} - F_{cr2}\right) \cdot h_c + F_v \cdot h_v \Big] \Big/ L_r, \end{aligned} \quad (2.\ 13)$$

A particularly important role in the stability of the movement of the convoy, in longitudinal direction, is played by the **braking**. The braking moments are established by multiplying the values of the normal dynamic reactions, corresponding to each axle, with the value of the coefficient of friction at slip and with that of the wheel radius.

Details on the construction and calculation of the braking systems are presented in **[27].**

2. 2. 2. Moving in a curve

Figures 2. 2… 2. 4 show the phases of joining a curve of a transport system with articulated trailers.

Case 1. ***The pulling module enters the curve*** (fig. 2. 2) **[6, 29].** The centers of mass are considered to be in the middle of the transportation modules (where the pivoting supports are also located), respectively in the middle of the bridge supporting the transported load. The equation of the bending moment with respect to the pivot of the pulling module is written in the form:

$$F_{cr1}\cdot L_p\cdot\sin\alpha_c - Y_1\cdot L_p\cdot\cos\theta_m + 2\cdot M_{p1} = 0, \tag{2. 15}$$

$$M_{p1} = F_{cr1}\cdot l_p\cdot sin\alpha_c;\ \theta_m = \mathrm{arctan}\left(0{,}5\cdot L_p / R\right);\ Y_1 = Z_{f1}\cdot\sqrt{\varphi^2 - f^2}, \tag{2. 16}$$

Case 2. ***The pulling module entered the curve*** (fig. 2. 3) **[6, 29].** Considering the angular velocity of the center of mass of the puller module equal to $\omega_m = v / R$ and its linear velocity *v* equal to the speed of the bridge (and the load) results:

$$\mathrm{d}\theta_2 / \mathrm{d}t = \omega_p = \omega_m + \mathrm{d}\theta_1 / \mathrm{d}t;\quad \mathrm{d}\omega_p / \mathrm{d}t = \mathrm{d}\omega_m / \mathrm{d}t + \mathrm{d}^2\theta_1 / \mathrm{d}t^2 = \mathrm{d}^2\theta_2 / \mathrm{d}t^2. \tag{2. 21}$$

Case 3. ***The convoy is in a curve*** (fig. 2. 4) **[6, 29].** In this situation the relative position between the transport modules and the bridge is stabilized, reason why $M_{f1} = M_{f2} = 0$. From the equilibrium equations of the bending moments in relation to points *A* and *B* (fig. 2. 4) it results:

$$\left\{F^{\bullet}_{cr1}, F^{\bullet}_{cr2}\right\}^{-1} = \left[A^{\bullet}\right]^{-1}\cdot\left\{B^{\bullet}\right\}, \tag{2. 30}$$

where:

$$\left[A^{\bullet}\right] = \begin{bmatrix} l_p\cdot\sin\alpha_c + 0{,}5\cdot L_p\cdot\sin\left(\gamma_1+\alpha_c\right) & l_p\cdot\sin\beta_c + L_r\cdot\cos\beta_c + \\ & +0{,}5\cdot L_p\cdot\sin\left(\gamma_1+\beta_c\right) \\ l_p\cdot\sin\alpha_c + L_r\cdot\cos\alpha_c + & \\ +0{,}5\cdot L_p\cdot\sin\left(\gamma_1+\alpha_c\right) & l_p\cdot\sin\beta_c + 0{,}5\cdot L_p\cdot\sin\left(\gamma_1+\beta_c\right) \end{bmatrix}; \tag{2. 31}$$

$$\{B\}=\begin{Bmatrix} -M_{iz1}-M_{iz2}-M_{izp}+0,5\left(Y_1+Y_2\right)\cdot L_p\cdot\cos\theta_m-0,5\cdot F_{inp}\cdot L_r+ \\ +\left(Y_3+Y_4\right)\cdot\left(0,5\cdot L_p\cdot\cos\theta_m-L_r\cdot\sin\gamma_1\cdot\sin\theta_m\right)+F_{it2}\cdot L_r\cdot\sin\gamma_1- \\ -F_{in2}\cdot L_r\cdot\cos\gamma_1+\left(Y_3-Y_4\right)\cdot L_r\cdot\cos\gamma_1\cdot\cos\theta_m \\ \hline -M_{iz1}-M_{iz2}-M_{izp}+0,5\cdot\left(Y_3+Y_4\right)\cdot L_p\cdot\cos\theta_m+0,5\cdot F_{inp}\cdot L_r- \\ -\left(Y_1+Y_2\right)\cdot\left(L_r\cdot\sin\gamma_1\cdot\sin\theta_m-0,5\cdot L_p\cdot\cos\theta_m\right)+F_{it2}\cdot L_r\cdot\sin\gamma_1+ \\ +F_{in2}\cdot L_r\cdot\cos\gamma_1+\left(Y_1-Y_2\right)\cdot L_r\cdot\cos\gamma_1\cdot\cos\theta_m \end{Bmatrix}. \quad (2.32)$$

2. 5. Conclusions and perspectives

The complete safety in the operation of equipment in the process industries, in general, of great complexity, and of the oversized ones, with high masses, in particular, is dependent on the compliance with standard conditions, on the behavior of the working parameters, chemically and / or mechanically aggressive substances, at low or high pressures, as well as negative or high temperatures. Design has an essential role in the chain of activities (choosing the appropriate construction materials, but technically and economically competitive, the influence of the foundation ground behavior, tectonic behavior, meteorological loads), as well as fabrication, transportation and stable operation. In order to preserve the geometric characteristics of the transported equipment, a careful analysis of the stages of their movement is required **[44 - 46],** starting with their proper fixing on platforms and continuing with longitudinal and transverse stability, on roads with low inclinations.

In this sense, in this chapter we study the calculation of the towing forces of a convoy for transport with two distant platforms, of an oversized mechanical equipment, in a straight line or in curves. It is also offered the way to appreciate the geometry of the curved route, in the case previously expressed. The routes are considered without unevenness, the transversal inclination of the roads being neglected.

As perspectives, are considered:

- more steep slopes, even with unevenness (inside the construction sites, for example) and various travel regimes;
- analysis of joining the curves with variable speed, considering the characteristics of the surface and the transversal inclination;
- analysis of the variable influence of the effects of wind loads;
- assessment of the entrances and exits of the transport platforms, respectively the trajectories on which the towing vehicles travel;
- the influence of the special vibrating regime that appears on the uneven roads, especially inside the construction sites, both on the driver / drivers and on the load.

CHAPTER 3

CONSIDERATIONS REGARDING THE LONGITUDINAL STABILITY OF THE TRANSPORT MOVEMENT OF OVERSIZED TECHNOLOGICAL EQUIPMENT

3. 1. Introduction

This chapter addresses the conditions necessary to ensure the stability of the longitudinal movement of towing vehicles such as wheeled or tracked vehicles and platforms loaded with oversized mechanical equipment.

3. 2. Means for towing

Among the performance of the vehicles, the most important are: maximum speed, acceleration capacity at start (the start-up time and space, acceleration, average travel speed), the ability to climb or descend slopes, braking capacity (when a transient regime of vehicle movement is manifested, by reducing the speed to a certain value or to the rest state) **[4 - 6].**

3. 2. 1. Vehicles with tires

Normal reactions in the area of contact of the wheels with the road have a special role on their adhesion to the road surface, with implications in achieving the stability of vehicles. These reactions have values determined by the static distribution of the vehicle mass (with and without working load) on wheels, state that depends on the position of the center of mass and the inclination of the road to the horizontal.

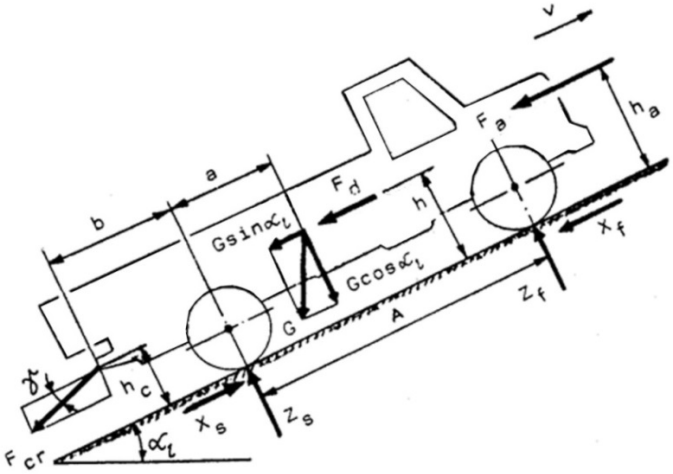

Fig. 3. 1. Diagram for assessing the longitudinal stability of a truck when climbing the slope **[16].**

3. 2. 1. 1. Two-axle trucks

In the case of **a truck ascending a slope / ramp**, in a regime of accelerated movement (fig. 3. 1), the normal reactions have the expressions:

$$Z_f = \frac{1}{A}\cdot\left[G\cdot\left(a\cdot\cos\alpha_l - h\cdot\sin\alpha_l\right) - F_{cr}\cdot\left(h_c\cdot\cos\gamma + b\cdot\sin\gamma\right) - F_a\cdot h_a - F_d\cdot h^*\right];$$

$$Z_s = \frac{1}{A}\cdot\left\{G\cdot\left[\left(A-a\right)\cdot\cos\alpha_l + h\cdot\sin\alpha_l\right] + F_{cr}\cdot\left[h_c\cdot\cos\gamma + \left(A+b\right)\cdot\sin\gamma\right] + F_a\cdot h_a + F_d\cdot h^*\right\}, \quad (3.\ 1)$$

Overturning around the rear wheels can occur when the sum of the overturning moments relative to the center of mass exceeds the sum of the stabilizing moments, ie:

$$F_{cr}\cdot\left[-\left(h-h_c\right)\cdot\cos\gamma+\left(a+b\right)\cdot\sin\gamma\right]+F_d\cdot\left(h^*-h\right)+F_a\cdot\left(h_a-h\right)+$$
$$+Z_f\cdot\left(A-a\right)+X_s\cdot h\ \geq\ X_f\cdot h+Z_s\cdot a\,, \tag{3. 2}$$

Danger of the truck tipping over when it **descends on a slope** around the front wheels occurs when it has a steep inclination. The descent is usually performed with the truck braked, so at low speed. Until the wheels are completely locked (fig. 3. 2) the friction forces of the wheels with the road surface meet the conditions:

$$F_{fs}\leq\varphi_p\cdot Z_s\,;\quad F_{ff}\leq\varphi_p\cdot Z_f\ . \tag{3. 12}$$

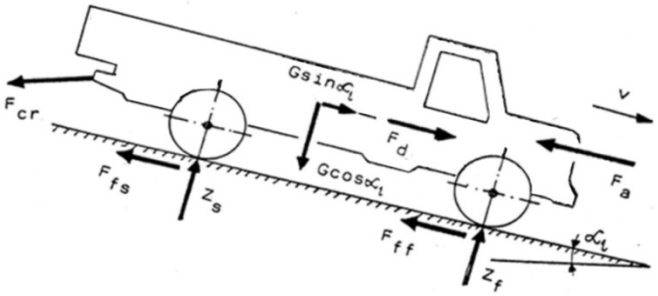

Fig. 3. 2. Diagram for assessing the longitudinal stability of a vehicle, when descending the slope **[16].**

The danger of **overturning** around the front wheels occurs when:

$$F_d\cdot\left(h^*-h\right)+\ Z_s\cdot a\ +\ F_{fs}\cdot h\ +\ F_{cr}\cdot\left(\ h\ -\ h_c\right)\cdot\cos\gamma+\ F_{ff}\cdot h\ \geq$$
$$\geq\ F_a\cdot\left(\ h_a\ -h\right)\ +\ Z_f\cdot\left(A-a\right)+F_{cr}\cdot\left(\ a\ +\ b\ \right)\cdot\sin\gamma\,, \tag{3. 15}$$

3. 2. 1. 2. Three-axle trucks

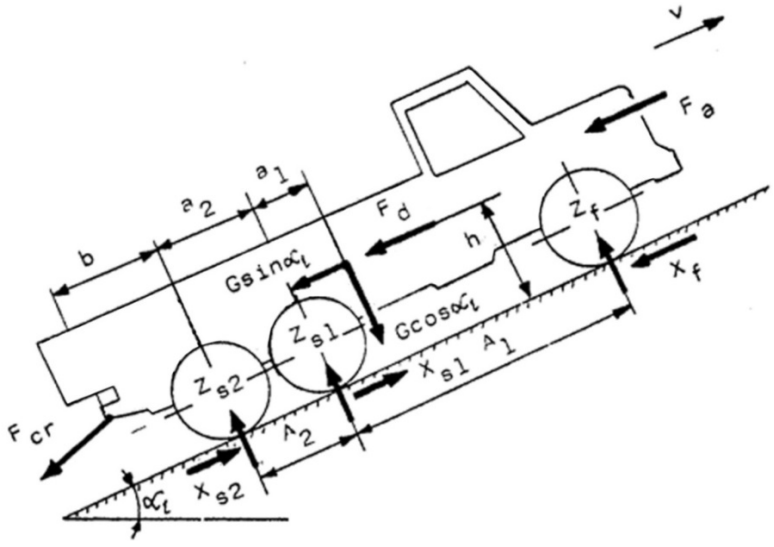

Fig. 3. 3. Diagram for assessing the longitudinal stability of a three-axle truck **[16]**

These vehicles generally have rear drive axles (fig. 3.3) and sometimes the possibility to engage the front axle, which also becomes a dive axle. The suspension of the rear axles is made in two variants, more common: with semi-elliptical springs and reaction bars. The rear drive axles are connected to each other on each side of the truck by a rocker arm, which can oscillate around a joint, integral with the chassis and arranged transversely.

The loss of longitudinal stability of the truck occurs when:

$$\begin{aligned} &F_d\cdot\left(h^*-h\right)+F_a\cdot\left(h_a-h\right)+F_{cr}\cdot\left(a_1+a_2+b\right)\cdot\sin\gamma+Z_f\cdot\left(A_1-a_1\right)+\\ &+\left(Z_{s1}+Z_{s2}\right)\cdot\varphi_p\cdot h\geq Z_{s1}\cdot a_1+Z_{s2}\cdot\left(a_1+a_2\right)+F_{cr}\cdot\left(h-h_c\right)\cdot\cos\gamma+\varphi_p\cdot Z_f \end{aligned}, \quad (3.\ 27)$$

When descending a slope in a braked regime, the danger of overturning around the front wheels occurs when,

$$\begin{aligned} &F_d\cdot\left(h^*-h\right)+\left(F_{ff}+F_{fs1}+F_{fs2}\right)\cdot h+F_{cr}\cdot\left(h-h_c\right)\cdot\cos\gamma+Z_{s1}\cdot a_1+\\ &+Z_{s2}\cdot\left(a_1+a_2\right)\geq F_a\cdot\left(h_a-h\right)+Z_f\cdot\left(A_1-a_1\right)+F_{cr}\cdot\left(a_1+a_2+b\right)\cdot\sin\gamma, \end{aligned} \quad (3.\ 29)$$

3. 2 . 1. 3. Wheeled tractors with tires

The forces acting on a wheeled tractor (4 × 2), are indicated in figure 3. 4, keeping the same meanings as in figures 3. 1 and 3. 2:

a) deformable wheels on a rigid surface (concrete or asphalted roads);

b) deformable wheels on a deformable surface, the most typical case for wheeled tractors with tires.

When **descending the slope**, **overturning** can occur when:

$$\begin{aligned} &F_{fs}\cdot h+F_{cr}\cdot\left(h-h_c\right)\cdot\cos\gamma+Z_s\cdot\left(a-a_s\right)+F_d\cdot\left(h^*-h\right)+F_{ff}\cdot\left(h-t_t\right)\geq\\ &\geq F_a\cdot\left(h_a-h\right)+F_{cr}\cdot\left(a+b\right)\cdot\sin\gamma+Z_f\cdot\left(A-a+a_f\right), \end{aligned} \quad (3.\ 35)$$

measuring from the direction of the force F_a to the direction of the force X_s.

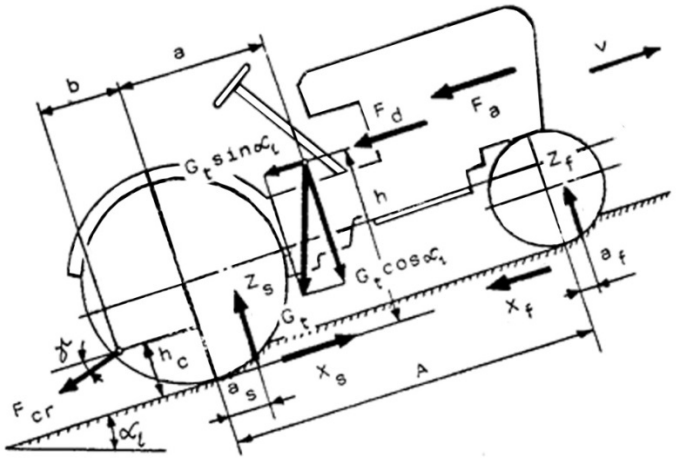

Fig. 3. 4. Diagram for assessing the longitudinal stability of a wheeled tractor when climbing a slope **[9, 16].**

For 4 x 4 tractors, the problem of longitudinal motion stability is treated similarly to that of two-axle trucks. Tractoarele de formula 4 × 4 se împart în două categorii:

a) with four drive wheels unequal in;

b) four wheels equal in diameter and with articulated chassis (thus increasing the possibility of turning at lower radii).

3. 2. 2. Tracked tractors

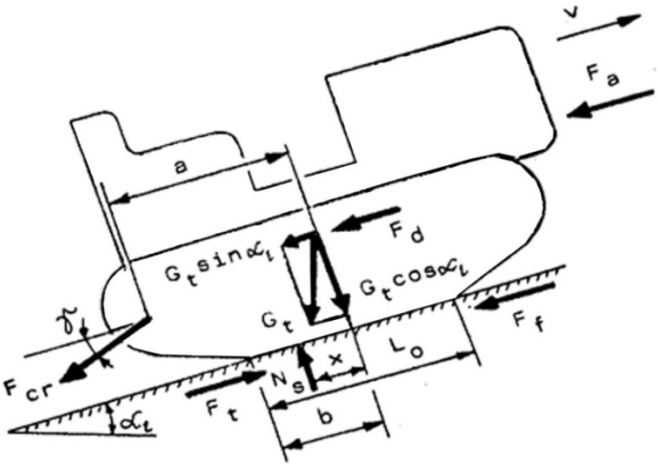

Fig. 3. 5. Diagram for assessing the longitudinal stability of a tracked tractor **[9, 16]**

In the case of **climbing a ramp** (fig. 3 .5), in accelerated motion, the three equilibrium equations are presented in the form:

$$F_t - F_f - F_{cr} \cdot \cos\gamma - G_t \cdot \sin\alpha_l - F_d - F_a = 0; \quad (3.\ 36)$$

$$N_s - F_{cr} \cdot \sin\gamma - G_t \cdot \cos\alpha_l = 0; \quad (3.\ 37)$$

$$G_t \cdot h \cdot \sin\alpha_l + F_d \cdot h + F_{cr} \cdot h_c \cdot \cos\gamma + F_a \cdot h_a + F_{cr} \cdot a \cdot \sin\gamma + M_{it} - N_s \cdot x = 0, \quad (3.\ 38)$$

The danger of **overturning** the crawler tractor when climbing the ramp exists when:

$$G_t \cdot h \cdot \sin\alpha_l + F_d \cdot h + F_a \cdot h_a + F_{cr} \cdot \left[h_c \cdot \cos\alpha_l + \left(a - b \right) \cdot \sin\alpha_l \right] \geq G_t \cdot b \cdot \cos\alpha_l. \quad (3.\ 42)$$

When **descending the slope**, in braking mode, the loss of longitudinal stability occurs when:

$$\begin{gathered} \left(G_t \cdot \sin\alpha_l + F_d \right) \cdot h \geq \\ \geq F_a \cdot h_a + F_{cr} \cdot \left[h_c \cdot \cos\gamma + \left(a - b + L_0 \right) \cdot \sin\gamma \right] + G_t \cdot \left(L_0 - b \right) \cdot \cos\alpha_l. \end{gathered} \quad (3.\ 43)$$

3. 3. Longitudinal movement stability of loaded platforms

3. 3. 1. Introduction

The following loads act on the load - vehicle assembly during uniform movement: force due to wind action, centrifugal force (when cornering), own weight and components of towing forces.

3. 3. 2. Stability of movement when climbing the slope

3. 3. 2. 1. Transportation with two distant platforms

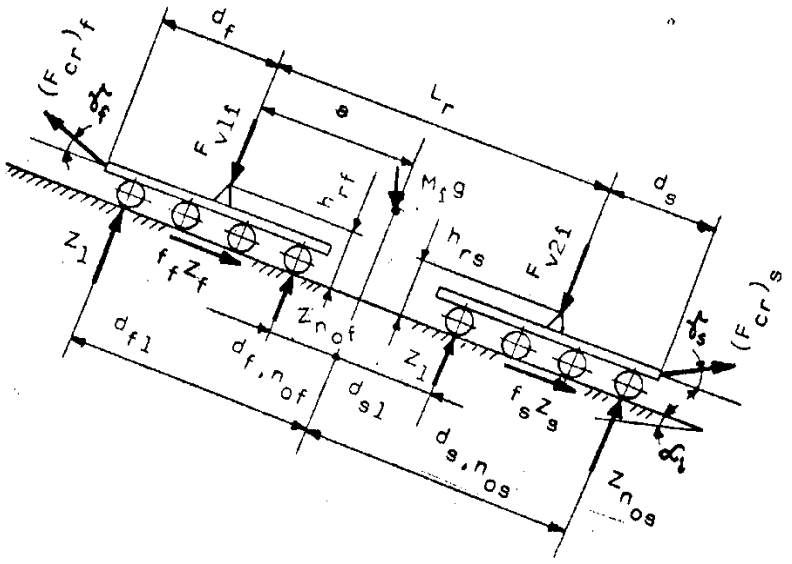

Fig. 3. 6. Sketch on the study of the longitudinal stability of an equipment transported on two distant platforms - the ***ascent of the ramp / slope*** **[9]**

Consider the support of the equipment on two pivoting supports (fig.3.6), resulting in the expressions of the normal reactions, $F_{v1\hat{i}}$ (acting on the front platform), respectively $F_{v2\hat{i}}$ (corresponding to the rear platform), N, written in the forms:

$$F_{v1\hat{i}} = \frac{1}{L_r + \mu_r \cdot \left(h_{rf} - h_{rs}\right)} \cdot \left\{ M_{\hat{i}} \cdot g \cdot \left[\left(L_r - a\right) \cdot \cos\alpha_l - \left(H_{c\hat{i}1} - h_{rs}\right) \cdot \sin\alpha_l \right] - \right.$$

$$\left. - F_{v\hat{i}l} \cdot \left(H_{v\hat{i}1} - h_{rs}\right) - F_{i\hat{i}l} \cdot \left(H_{c\hat{i}1} - h_{rs}\right) \right\}; \qquad (3.47)$$

$$F_{v2\hat{i}} = \frac{1}{L_r + \mu_r \cdot \left(h_{rf} - h_{rs}\right)} \cdot \left\{ M_{\hat{i}} \cdot g \cdot \left[\left(H_{c\hat{i}1} - h_{rf}\right) \cdot \sin\alpha_l + a \cdot \cos\alpha_l \right] + \right.$$

$$\left. + F_{v\hat{i}l} \cdot \left(H_{v\hat{i}1} - h_{rf}\right) + F_{i\hat{i}l} \cdot \left(H_{c\hat{i}1} - h_{rf}\right) \right\}, \qquad (3.48)$$

In order for the equipment not to move along its axis, it is necessary that:

$$\mu_r \cdot M_{\hat{i}} \cdot g \cdot \cos\alpha_l \geq M_{\hat{i}} \cdot g \cdot \sin\alpha_l + F_{ivl} + F_{v\hat{i}l}. \qquad (3.52)$$

The condition of overturning stability of the whole assembly (platforms - load) is presented by the inequality:

$$c_s \cdot \left\{ F_{vlT} \cdot \left(H_{v1} - H_{c1}\right) + \left(F_{cr}\right)_f \cdot \left[k_{crf} \cdot \left(L_{pp} + d_f + a\right) \cdot \sin\gamma_f + \right.\right.$$

$$+\left(H_{c1}-h_{cf}\right)\cdot\cos\gamma_f\Big]+\sum_{i=1}^{n_{0f}}Z_i\cdot d_{fi}\Big\}\le\left(f_f\cdot Z_f+f_s\cdot Z_s\right)\cdot H_{c1}+$$

$$+\left(F_{cr}\right)_s\cdot\Big[k_{crs}\cdot\left(L_{pps}+d_s-L_r+a\right)\cdot\sin\gamma_s+\left(H_{c1}-h_{cs}\right)\cdot\cos\gamma_s\Big]+\sum_{i=1}^{n_{0s}}Z_i\cdot d_{si}\,, \tag{3.53}$$

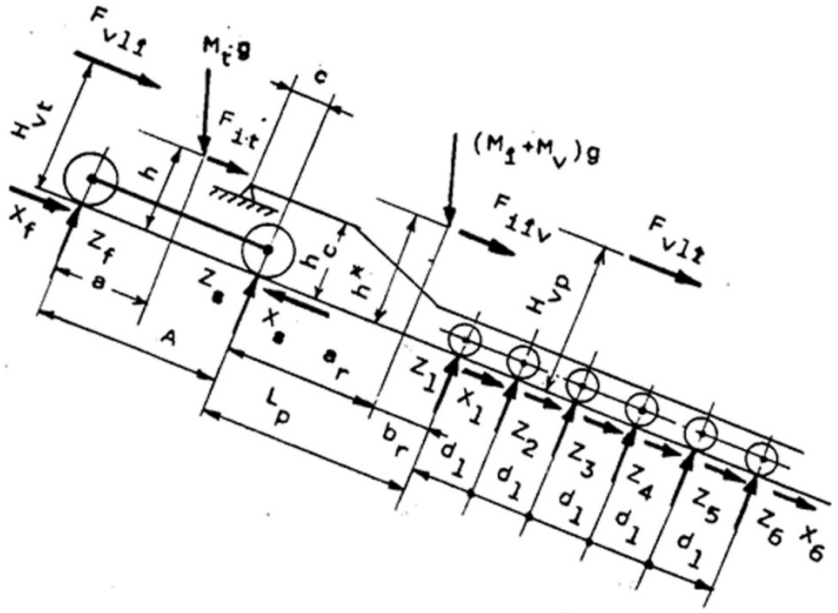

Fig. 3. 7. Scheme regarding the study of the transportation stability with semi-trailers with equidistant axles **[9]**

3. 3. 2. 2. Transportation with semi-trailers [9]

3. 3. 2. 2. 1. Deformation of the suspension and tires is neglected

With the notations in figure 3. 7 the following expressions are established for the reactions characteristic of the axles of the towing means:

$$Z_f=\left(a/A\right)\cdot M_t\cdot g\cdot\cos\alpha_l+\left(M_2/A\right); \tag{3.54}$$

$$Z_s=\left[\left(1-\frac{a}{A}\right)\cdot M_t+\frac{a_r-c}{L_p-c}\cdot\left(M_{\hat{i}}+M_v\right)\right]\cdot g\cdot\cos\alpha_l-\frac{M_2}{A}+\frac{M_3-M_2}{L_p-c}, \tag{3.55}$$

The expressions of the reactions corresponding to the axles of the semi-trailer are presented in the forms:

$$Z_{1/6}=Z_{1/5};\quad Z_{2/6}=Z_{2/5};\quad Z_{3/6}=Z_{3/5};\quad Z_{4/6}=\left(M_5-2M_6+M_7\right)/d_1; \tag{3.56}$$

$$Z_{5/6}=\left(M_6-2M_7\right)/d_1;\quad Z_{6/6}=M_7/d_1, \tag{3.57}$$

3. 3. 2. 2. 2. Deformation of the suspension and tires is not neglected

The safety of the convoy movement is guaranteed when:

$$c_s \cdot \left[F_{vl\hat{i}} \cdot \left(H_{vt} - H_{ts} \right) + F_{vlt} \cdot \left(H_{vp} - H_{ts} \right) + Z_f \cdot L_{ts} + \right.$$

$$\left. + Z_s \cdot \left(L_{ts} - A + \varphi_p \cdot H_{ts} \right) \right] \leq \left(f_f \cdot Z_f + f \cdot \sum_{i=1}^{n_0} Z_i \right) \cdot H_{ts} +$$

$$+ \sum_{i=1}^{n_0} Z_i \cdot \left[L_p \, A - L_{ts} + \left(i - 1 \right) \cdot d_1 \right], \qquad (3.71)$$

3. 3. 3. Stability of movement when descending the slope

Accepting that in this situation the convoy consisting of the towing vehicle and the loaded semi-trailer is braked, reactions Z_f and Z_s (fig.3. 7) is determined by formulas of the type (3. 54).

Sliding to the foot of the slope is not possible, under the conditions expressed in relation (3. 71) when:

$$\left(M_t + M_{\hat{i}} + M_v \right) \cdot \left(g \cdot \sin \alpha_l + dv / dt \right) + \varphi_p \cdot Z_s \leq F_{vlt} + F_{vl\hat{i}} + f_f \cdot Z_f + f \cdot \sum_{i=1}^{n_0} Z_i \qquad (3.75)$$

while **the overturning** does not take place if:

$$c_s \cdot \left\{ \sum_{i=1}^{n_0} Z_i \cdot \left[L_p + A - L_{ts} + \left(i - 1 \right) \cdot d_1 \right] + \left(f_f \cdot Z_f + f \cdot \sum_{i=1}^{n_0} Z_i \right) \cdot H_{ts} \right\} \leq$$

$$\leq F_{vl\hat{i}} \cdot \left(H_{vt} - H_{ts} \right) + F_{vlt} \cdot \left(H_{vp} - H_{ts} \right) + Z_f \cdot L_{ts} + Z_s \cdot \left(L_{ts} - A + \varphi_p \cdot H_{ts} \right). \qquad (3.76)$$

3. 4. Conclusions and perspectives

In the previous statements, the expression of the conditions regarding the stability of the longitudinal movement of the single or loaded vehicles, respectively of the loaded platforms, when ascending or descending the ramp was taken into account. It is specified the appropriate data for two remote platforms and semi-trailers. The effects of dynamic loads on acceleration or braking, as well as the influence of wind, are not neglected.

As **perspectives** can be considered:

- The analysis of the movement behavior on rough roads, along the adopted routes or inside the construction sites;
- The stability of the longitudinal movement of multi-axle vehicles;
- Correct evaluation of all loads that occur in the anchor points, for sizing or checking the geometry of the ears, respectively the buttons.

CHAPTER 4

SOME ASPECTS REGARDING THE TRANSVERSAL STABILITY OF THE MOVEMENT OF PLATFORMS LOADED WITH OVERSIZED TECHNOLOGICAL EQUIPMENT

4. 1. Introduction

As in the case of the longitudinal stability of the movement of road vehicles, single or combined with the platforms for transporting oversized industrial equipment, in this case the necessary conditions for the stability in the transverse direction of the convoys are taken into account **[1 - 7].** The possible insecurity in this situation is manifested by **skidding** (lateral slip) or by **overturning** (around the line joining the points of contact of the wheels on the same side) to the base of the slope or inside the curve.

4. 2. Wheeled vehicles

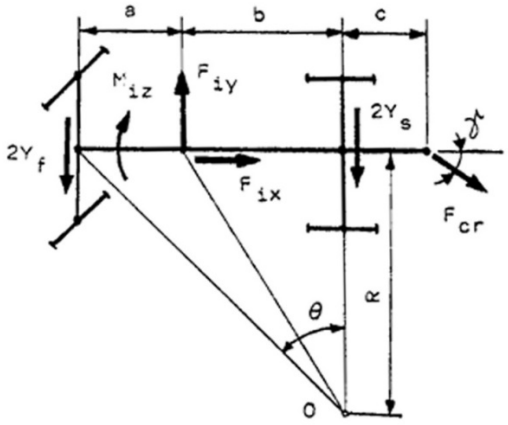

Fig. 4. 1. Sketch for calculating the loads developed on vehicles traveling in curves **[9]**

In many situations, for real reasons, there may be an uneven and curvilinear movement of the vehicles, with changes in the steering angle. In this case, inertia forces caused by the mass of the vehicle develop, respectively moments corresponding to the inertia of the rotating masses (fig. 4. 1) **[8]:**

$$F_{ix} = (G/g)\cdot\left[(dv/dt) - b\cdot(v^2/R^2)\right]; \tag{4. 1}$$

$$F_{iy} = (G/g)\cdot\left[(v^2/R) + (b/R)\cdot(dv/dt)\right]; \tag{4. 2}$$

$$M_{iz} = \left[(G\cdot\rho_z^2)/(g\cdot R)\right]\cdot(dv/dt), \tag{4. 3}$$

To evaluate the values of the transverse reactions (fig. 4. 1) the condition of dynamic equilibrium of the bending moments around the midpoints of the front and rear axles will be expressed, establishing the equalities:

$$Y_f = \frac{b\cdot\left[\left(F_{iy} + F_v^*\right)\cdot\cos\alpha_t - G\cdot\sin\alpha_t\right] + c\cdot F_{cr}\cdot\sin\gamma + M_{iz}}{2\cdot(a+b)}; \tag{4. 7}$$

$$Y_s = \frac{a\cdot\left[\left(F_{iy}+F_v^*\right)\cdot\cos\alpha_t - G\cdot\sin\alpha_t\right]-\left(a+b+c\right)\cdot F_{cr}\cdot\sin\gamma - M_{iz}}{2\cdot\left(a+b\right)}, \qquad (4.\ 8)$$

Transverse overturning during cornering may occur when the condition is met $2\cdot Z_s \geq 0$, from where it is established, following the calculations,

$$\tan\alpha_t \geq \left[2\cdot h\cdot\left(F_{iy}+F_v^*\right)-B\cdot G\right] \Big/ \left[2\cdot h\cdot\left(F_{iy}+F_v^*\right)+B\cdot G\right]. \qquad (4.\ 13)$$

4. 3. Tracked vehicles

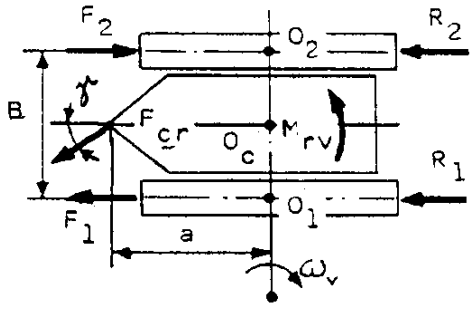

Fig. 4. 3. Stresses of a vehicle with tracks in the corner **[2]**

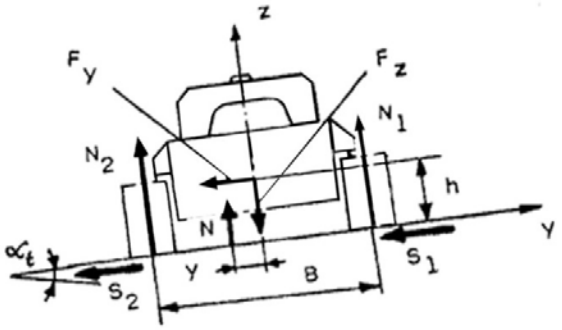

Fig. 4. 4. Sketch for the study of the transverse stability of tracked vehicles **[9]**

When the tracks advance on a certain route, a vertical deformation of the ground occurs, resulting in forward resistance forces R_1 and R_2 (fig. 4. 3). The twisting moment is created in the turning process M_{rv}, respectively the forces F_1 and F_2 produced on the front tracks, different from each other only in value, or as value and direction (in correspondence with the type of steering mechanism). From the equilibrium equations of the bending moments in relation to points O_1 and O_2 (fig. 4. 3) the equalities are deduced:

$$\begin{aligned} F_1 &= -R_1 + M_{rv}/B + \left[\left(a/B\right)\cdot\sin\gamma - 0{,}5\cdot\cos\gamma\right]\cdot F_{cr}; \\ F_2 &= R_2 + M_{rv}/B + \left[\left(a/B\right)\cdot\sin\gamma + 0{,}5\cdot\cos\gamma\right]\cdot F_{cr}, \end{aligned} \qquad (4.\ 14)$$

Considering figure 4. 4, it is written the equilibrium equations of forces and bending moments:

$$F_y - \left(S_1+S_2\right)=0; \quad N - F_z = 0; \quad F_y\cdot h - N\cdot y = 0, \qquad (4.\ 15)$$

with the appropriate expressions

$$F_y = -G_t\cdot\sin\alpha_t + F_v^*\cdot\cos\alpha_t + F_c; \qquad (4.\ 16)$$

$$F_z = G_t\cdot\cos\alpha_t + F_v^*\cdot\sin\alpha_t; \qquad (4.\ 17)$$

$$S_1 + S_2 = \mu\cdot\left(N_1+N_2\right) = \mu\cdot N. \qquad (4.\ 18)$$

With the help of expressions (4. 15), from equality (4. 18) is obtained:

$$y = \left[\left(G_t\cdot\sin\alpha_t - F_v^*\cdot\cos\alpha_t - F_c\right) \Big/ \left(G_t\cdot\cos\alpha_t + F_v^*\cdot\sin\alpha_t\right)\right]\cdot h. \qquad (4.\ 19)$$

Overturning can occur when $y = B/2$ and therefore,

$$2 \cdot \left[\left(G_t \cdot \sin \alpha_t - F_v^* \cdot \cos \alpha_t - F_c \right) \Big/ \left(G_t \cdot \cos \alpha_t + F_v^* \cdot \sin \alpha_t \right) \right] \cdot \left(h / B \right) \leq 0 . \qquad (4.\ 20)$$

On the other hand, **slipping** can occur when:

$$F_v^* \cdot \cos \alpha_t + F_c - G_t \cdot \sin \alpha_t \geq \varphi_p \cdot \left(G_t \cdot \cos \alpha_t + F_v^* \cdot \sin \alpha_t \right). \qquad (4.\ 21)$$

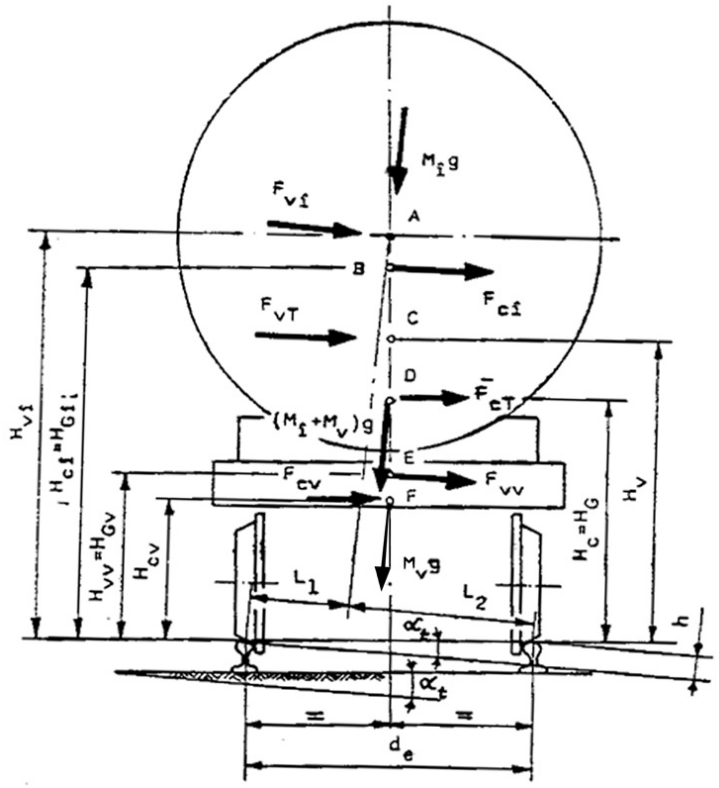

Fig. 4. 5. Sketch with the forces that stress the load-wagon assembly in curves, transversely to the equipment axis **[6, 9]**

4. 4. Loaded platforms

It is obvious that on the transport platforms, as well as on the load, act the mass forces, inertia forces, wind components, friction / adhesion forces to which are added, when in curves, centrifugal forces. Figures 4. 5 and 4. 6 show the forces mentioned and their points of application for transport on railways and roads. FCentrifugal forces have their application points in the centers of mass of the equipment (load), respectively of the platform. The calculation relations are presented in the forms:

$$F_{c\hat{i}} = M_{\hat{i}} \cdot v^2 \Big/ R_{\hat{i}} ; \qquad F_{cv} = M_v \cdot v^2 \Big/ R_v , \qquad (4.\ 22)$$

The total centrifugal force is determined with the help of equality:

$$F_{cT} = F_{c\hat{i}} + F_{cv} , \qquad (4.\ 23)$$

Wind forces can be established with expressions **[6, 9]:**

$$F_{v\hat{i}l} = 0{,}5 \cdot \beta \cdot C_t \cdot \rho_a \cdot v_v^2 \cdot A_{l\hat{i}} \cdot \sin^2 \beta_l = C_v \cdot A_{l\hat{i}} \cdot \sin^2 \beta_l , \qquad (4.\ 24)$$

for the transported load, respectively:

$$F_{vvl} = 0,5 \cdot \beta \cdot C_t \cdot \rho_a \cdot v_v^2 \cdot A_{lv} \cdot \sin \beta_l = C_v \cdot A_{lv} \cdot \sin \beta_l \ , \qquad (4.\ 25)$$

for the transport platform, where:

$$C_v = 0,5 \cdot \beta \cdot C_t \cdot \rho_a \cdot v_v^2 \ .$$

The total wind force that can act on the side surface of the load-platform assembly has the expression:

$$F_{vtT} = F_{vîl} + F_{vvl}, \qquad (4.\ 26)$$

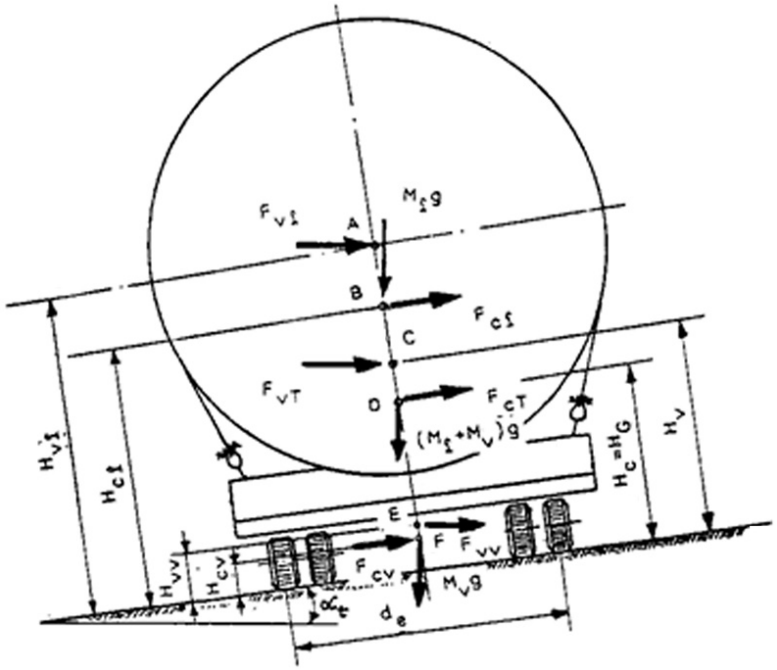

Fig. 4. 6. Sketch with the forces that stress the load-trailer assembly in curves, transversely to the equipment axis **[6, 9]**

The loss of stability of the transverse movement of the transport system may be manifested by **slipping or overturning laterally**, on straight or curved paths, caused by the simultaneous or individual action of centrifugal forces or lateral wind (for the particular case of railways must be taken into account their specific characteristics **[11 - 19]**).

In order for the load-vehicle assembly to run safely on public roads, the condition must be met:

$$c_s \cdot M_R \le M_S, \qquad (4.\ 27)$$

Taking into account the forces on the hook - front $\left(F_{cr}\right)_f$, respectively at the hook - back $\left(F_{cr}\right)_s$, the expressions result:

$$M_S = -\ 0{,}5 \cdot C_v \cdot \left(A_{l\hat{i}} + A_{lv} \right) \cdot d_e \cdot \sin\left(\beta_l - \theta \right) \cdot \sin \alpha_t +$$

$$+\ 0{,}5 \cdot \left(M_{\hat{i}} + M_v \right) \cdot g \cdot d_e \cdot \cos \alpha_t + \left[\left(F_{cr} \right)_f \cdot \cos \gamma_f \cdot \sin \alpha_{cf} + \right.$$

$$\left. + \left(F_{cr} \right)_s \cdot \cos \gamma_s \cdot \sin \alpha_{cs} \right] \cdot h_c ; \qquad (4.\ 28)$$

$$M_R = C_v \cdot \left(A_{l\hat{i}} + A_{lv} \right) \cdot H_V \cdot \sin\left(\beta_l - \theta \right) \cdot \cos \alpha_t -$$

$$- \left(M_{\hat{i}} + M_v \right) \cdot \left(g \cdot \sin \alpha_t - v^2 / R \right) \cdot H_c , \qquad (4.\ 29)$$

Based on inequality (4. 27) and taking into account the equalities (4. 28) and (4. 29) - with the safety factor $c_s = 1,5$ - the following wind speed limitation is obtained **[9]:**

$$v_{vr} \le \left[\sin\left(\beta_l - \theta \right) \right]^{-1} \cdot \sqrt{2 \cdot F_1 \Big/ \left[\begin{array}{c} \beta \cdot C_t \cdot \rho_a \cdot \left(A_{l\hat{i}} + A_{lv} \right) \cdot \\ \left(3 \cdot H_v \cdot \cos^2 \alpha_t + d_e \cdot \sin^2 \alpha_t \right) \end{array} \right]} \cdot \qquad (4.\ 30)$$

respectively, for the speed of the vehicle:

$$v \le \sqrt{F_2 \cdot R \Big/ \left[3 \left(M_{\hat{i}} + M_v \right) \cdot H_C \right]}, \qquad (4.\ 31)$$

Accepting that the transverse stability condition (4. 27) of the transportation platform-load assembly is met, with the bending moments established with the equalities (4. 28) and (4. 29), it is necessary to evaluate the developed reactions (obviously their maximum values).

$M_{vr} = \mu \cdot G_t \cdot L_0 / 4$ **[8];** μ - the coefficient of resistance of the soil to turning **[9].**

4. 6. Conclusions and perspectives

The previous presentation takes into account the conditions that allow the safe movement of vehicles or vehicle-load assemblies, under the action of the loads that occur, both those belonging to the assembly and the external ones (wind forces, centrifugal forces, road surface condition). From the analysis of the structure of the established inequalities it is ascertained the importance of the exact knowledge of the meteorological conditions, as well as of the configuration of the crossed route. On the other hand, a special role in the lateral stability is played by the distribution of the loads carried on the axles of the means of transport or of the respective platforms **[20]**, but also the maximum pressures created between the rails and the wheels **[2].**

The reality should not be neglected, namely that most of the external loads have variable values, which is why the analysis must be done thoroughly for extreme situations. In this way, the extremes of the loads that allow the development of research for the transfer of the loads at the anchorage points (perspectives) are established.

CHAPTER 5

CALCULATION ELEMENTS OF WELDED FLAT LUGS AND TRUNNIONS FOR LIFTING OR ANCHORING OVERSIZED INDUSTRIAL EQUIPMENT

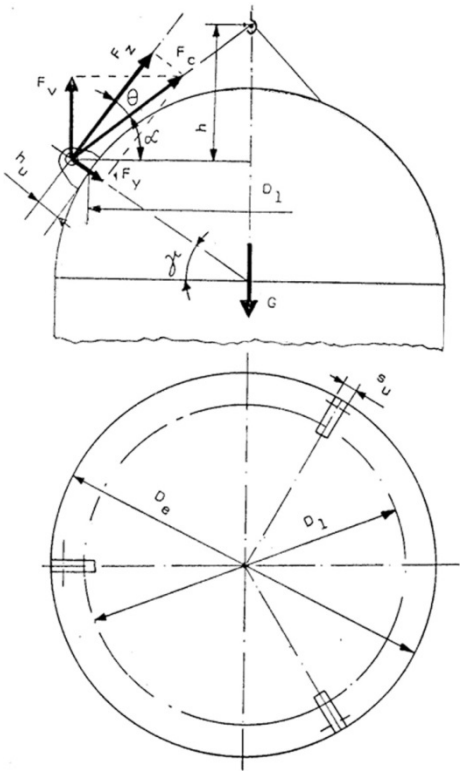

Fig. 5. 1. Placement of welded flat lugs on a hemispherical cover (sketch)

5. 1. Introduction

For the safety of the transport from the manufacturer to the beneficiary, a precise analysis of the maximum loads developed in the constructive elements for lifting or anchoring, such as cylindrical trunnions **[1, 9, 10]** or flat, welded, symmetrical or asymmetrical lugs **[11 - 22, 35, 36, 38 - 40, 43, 44]**, respectively other types (welded or screwed rings, double lugs, hooks) etc.[**15, 18].** The intensity of the stress states created both in the lifting or anchoring elements is assessed both analytically and by numerical and experimental methods, respectively on models or in site.

5. 2. Lugs used for lifting and handling vertical cylindrical equipment [1]

5. 2. 1. Spherical cover

It is envisaged to lift a vertical equipment, with a hemispherical cover, having the weight G , using symmetrical flat lugs, as shown in figure 5. 1, placed at 120^0 from each other. It is

easy to deduce that, for each lug, in the vertical position of the structure, the force F_v develops, with the relation:

$$F_v = G / n_u \ , \tag{5. 1}$$

The force in the lifting cables F_c, has the expression:

$$F_c = F_v / (sin\ \alpha) = G \cdot \sqrt{1 + tan^2 \alpha} \ / (n_u \cdot tan \alpha) \cdot \ , \tag{5. 2}$$

Tangential force F_z and radial force F_y have the expressions:

$$F_z = F_c \cdot \cos\theta ; \ F_y = F_c \cdot \sin\theta , \tag{5. 4}$$

where the angle $\theta = \pi / 2 - \gamma - \alpha$.

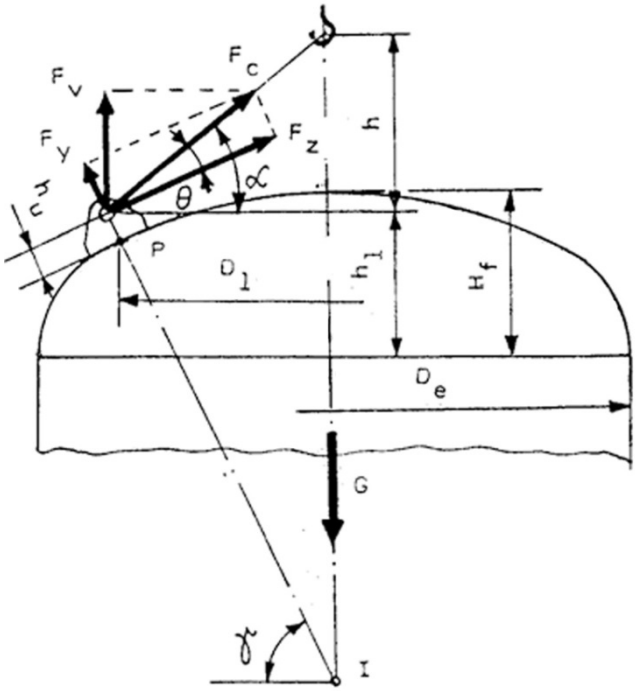

Fig. 5. 2. Placement of welded flat ears on a semi-ellipsoidal cover (sketch) **[1]**

5. 2. 2. Semi-ellipsoidal cover

In this situation it is easy to deduce that $\theta = \gamma + \alpha - \pi / 2$, where the angle α is calculated using equality (5. 3) $_1$, and the angle γ it is established using the relationship (fig. 5. 2):

$$sin\gamma = D_1 \cdot H_f \Big/ \sqrt{D_e^2 \cdot \left(D_e^2 - D_1^2 \right) + H_f^2 \cdot D_1^2} \ . \tag{5. 5}$$

5. 3. Flat lugs used for anchoring transported equipment

A way of anchoring a cylindrical equipment on the platform of a wagon is shown in figure 3.

The angle α from figure 5.3 can have the following values **[1]:**

► $\alpha \leq 45°$ for vesses with a diameter smaller than the width of the platform;

► $\alpha \leq 150°$ for vessels with a diameter larger than the width of the platform.

The lugs are fixed in the horizontal longitudinal plane (fig. 5. 4) - when the diameter of the equipment is smaller than the width of the platform - or below this plane, at an angle α (fig. 5. 5) - when the diameter of the equipment is larger than its width.

For sizing or checking the lugs, first determine the forces acting along the coordinate axes of the chosen reference system (fig. 5. 4 şi 5. 5):

► axis *A x*, parallel to the horizontal axis of the vessel;

► axis *A y*, along the radius of the vessel, located horizontally;

► axis *A z*, in the vertical direction.

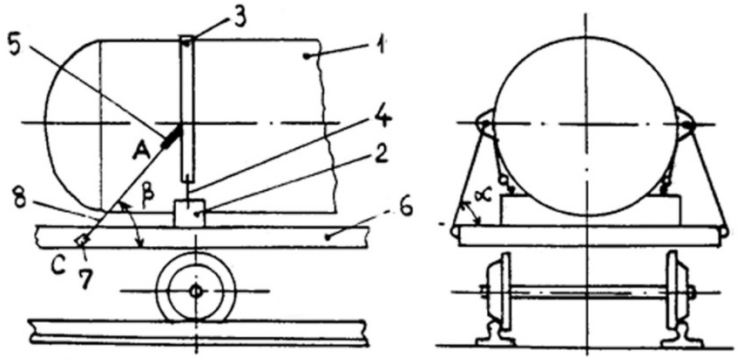

Fig. 5. 3. A way to anchor technological equipment on transport platforms (sketch) **[1]**
1- vessel; 2 – support; 3 – belt; 4 – fixing the belt to the platform; 5 – lug; 6 – platform (wagon or trailer); 7 – platform fixing point (eye); 8 – anchoring cable

5. 3. 1. Forces developed in the structure of a lug

5. 3. 1. 1. Sizing or checking the geometry of the lug [1]

The following hypotheses are considered:

► the effects introduced by the curvature of the external surface of the erected or anchored equipment in the area of fixation of the lug are neglected;

► the structure is considered as a non-deformable massif;

► the construction material of the lug is isotropic;

► the lug stress is in the elastic field;

► the forces are considered concentrated in their points of application;

► lifting and handling operations are done slowly, without shocks.

5. 3. 1. 1. 1. The diameter of the equipment is smaller than the width of the transport platform (fig. 5. 4)

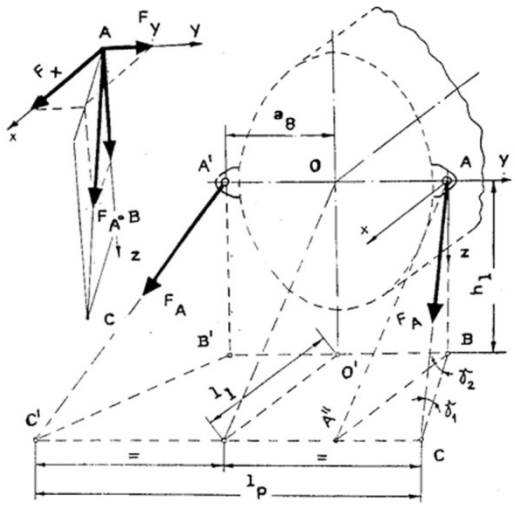

Fig. 5. 4. Anchoring equipment with an outside diameter smaller than the width of the transport platform (sketch) **[1]**

Accepting, as a first step, that the lugs are normal to the longitudinal axis of the transported equipment, the force F_A resulting from the tensioning of the anchors decomposes along the three axes of the reference system (where this time, axis *A y* is along the radius *O A*), as follows:

$$F_x = F_A \cdot \cos\gamma_1 \cdot \cos\gamma_2 ; F_y = F_A \cdot \cos\gamma_1 \cdot \sin\gamma_2 ; F_z = F_A \cdot \sin\gamma_1, \qquad (5.\ 6)$$

The state of tension developed by the components F_x, F_y, F_z at the base of the lug is illustrated by:

The effect of force F_x is found in the shear load **[23 - 25]** along the axis *A x* (fig. 5. 4), for which

$$\tau_x = \left[F_x / \left(s \cdot l_u \right) \right] \cdot \left(1{,}5 - 6\, x^2 / s^2 \right), \qquad (5.\ 8)$$

where $x \in [\,0\,;\ s/2\,]$ and the bending one due to the bending moment, the following tensions manifesting:

$$\sigma_x = \pm \left[12 \cdot M_x / \left(s^3 \cdot l_u \right) \right] \cdot x = \pm \left[12 \cdot F_x \cdot c / \left(s^3 \cdot l_u \right) \right] \cdot x, \qquad (5.\ 9)$$

oriented along the axis *A y*.

The effect of force F_y it is materialized in the tensile request reflected by the tension:

$$\sigma_y = F_y / \left(s \cdot l_u \right), \qquad (5.\ 10)$$

which also manifests along the axis *A y*.

The effect of force F_z it is felt in the shear reflected by the tension:

$$\tau_z = \left[F_z / \left(s \cdot l_u \right) \right] \cdot \left(1{,}5 - 6\, z^2 / l_u^2 \right), \qquad (5.\ 11)$$

where $z \in [\,0\,;\ s/2\,]$, manifested along the axis *A z*, as well as in the bending stress developed by the bending moment M_z, for which there are the following tensions:

$$\sigma_z = \pm\left[12 \cdot M_z \Big/ \left(s \cdot l_u^3\right)\right] \cdot z = \pm\left[12 \cdot F_z \cdot c \Big/ \left(s \cdot l_u^3\right)\right] \cdot z, \qquad (5.12)$$

acting along the axis *A y*.

The equivalent tension is calculated with the relation:

$$\sigma_{ech} = \sqrt{\left(\sigma_x + \sigma_y + \sigma_z\right)^2 + 3\left(\tau_x^2 + \tau_z^2\right)}, \qquad (5.13)$$

Using the appropriate stress expressions, the formula (5.13) becomes:

$$\sigma_{ech} = \left[1 \Big/ \left(s \cdot l_u\right)\right] \cdot \sqrt{f(x, z)}, \qquad (5.14)$$

The maximum equivalent tension, developed in the simple lug, is determined by the relationship:

$$\sigma_{ech,M} = \max\left\{\sigma_{ech,2}; \sigma_{ech,5}; \sigma_{ech,7}; \sigma_{ech,8}; \sigma_{ech,z_1}\right\}, \qquad (5.20)$$

when $z_1 \in [0;\ l_u / 2]$, or

$$\sigma_{ech,M} = \max\left\{\sigma_{ech,2}; \sigma_{ech,5}; \sigma_{ech,7}; \sigma_{ech,8}\right\}, \qquad (5.21)$$

when $z_1 \notin [0;\ l_u / 2]$.

When checking the geometry of the ear, $\sigma_{ech,M} \le \sigma_{au}$, where σ_{au} is the allowable stress of the lug material.

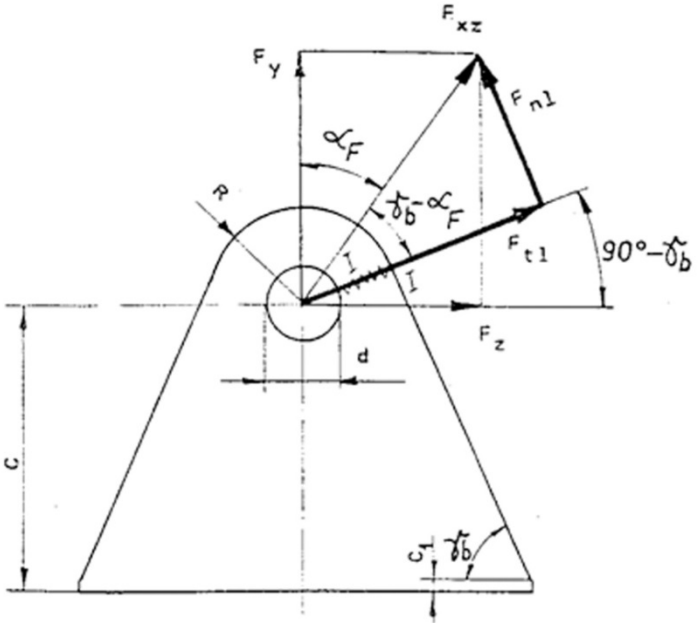

Fig. 5. 7. Loads for sizing or checking the geometry of the upper part of the lug (sketch)

Once the sizing or checking of the base of the lug is exhausted, the configuration of the upper area is chosen, taking into account the size of the anchor that passes through the eye, having the diameter d (fig. 5. 7).

The extension of the R-radius portion is verified by establishing the stress manifested in section I - I (fig. 5. 7):

► ***tensile force developed by*** F_{n1}:

$$\sigma_{1u} = \sqrt{F_y^2 + F_z^2} \cdot \sin\left(\gamma_b - \alpha_F\right) \Big/ \left[s \cdot \left(R - 0{,}5 \cdot d \right) \right]; \qquad (5.\ 22)$$

► ***shear produced by force*** F_{t1}

$$\tau_{1u} = \sqrt{F_y^2 + F_z^2} \cdot \cos\left(\gamma_b - \alpha_F\right) \Big/ \left[s \cdot \left(R - 0{,}5 \cdot d \right) \right], \qquad (5.\ 23)$$

The upper shape of the lug is accepted when:

$$\sqrt{\sigma_{1u}^2 + 3\tau_{1u}^2} \le \sigma_{au}. \qquad (5.\ 26)$$

5. 3. 1. 1. 2. The diameter of the equipment is larger than the width of the transport platform (fig. 5.8)

According to the reference system in figure 5.4, the force in the anchors decomposes into forces F_x, F_y, F_z which have the expressions (5. 6).

The forces necessary to calculate the state of tension, according to the methodology presented above, will have the expressions (the lug is normal to the axis of symmetry of the structure):

$$F_x = F_A \cdot \cos\gamma_1 \cdot \cos\gamma_2; \quad F_y = F_A \cdot \left(\sin\gamma_1 \cdot \sin\gamma + \cos\gamma_1 \cdot \sin\gamma_2 \cdot \cos\gamma \right); \quad F_z = F_A \cdot \left(\sin\gamma_1 \cdot \cos\gamma - \cos\gamma_1 \cdot \sin\gamma_2 \cdot \sin\gamma \right). \qquad (5.\ 29)$$

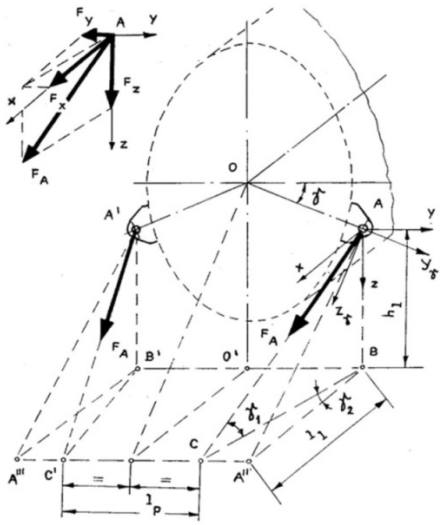

Fig. 5. 8. Anchoring equipment with an outside diameter greater than the width of the transport platform (sketch) **[1]**

5. 4. Trunnions for anchoring equipment [1, 35, 37, 45]

An alternative solution for anchoring technological equipment on transport platforms is by using trunnions, fixed directly to the equipment or by means of stiffening plates (there may also be combined solutions of lugs - trunnions, the trunnions being used, for example, to lift the equipment on foundations).

5. 4. 1. The diameter of the equipment is smaller than the width of the platform

5. 4. 1. 1. Sizing or checking the trunnion tube (pipe)

Within the study of the developed stresses, the simplified hypotheses accepted for the calculation of simple lugs for anchoring are kept here as well.

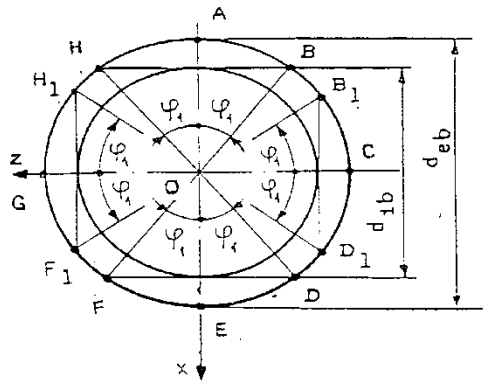

Fig. 5. 13. Diagram for calculation of the shear stresses in the trunnion tube **[1]**

► ***The effect of force*** F_x is found in the shear stress, for which:

$$\tau_{x1} = \left[\left(1{,}7 \cdot d_{eb}^{\,2} \cdot \sin^2 \varphi \right) \Big/ \left(d_{eb}^{\,4} - d_{ib}^{\,4} \right) \right] \cdot F_x , \qquad (5.\,52)$$

The bending stress given by the moment $M_x = F_x \cdot a_9$, where a_9 is the arm of component F_x in relation to the plane of fixing the trunnion to the body of the vessel (fig. 5. 12), is defined by the linear variation of the normal tensions that have the maximum values:

$$\sigma_{x0} = \pm\, 32 \cdot M_x \,/\, f_b , \qquad (5.\,54)$$

► ***The effect of force*** F_y (fig. 5. 12) is found in the tensile stress expressed by:

$$\sigma_y = F_y \Big/ \left[\pi \cdot \left(d_{eb} - s_b \right) \cdot s_b \right]. \qquad (5.\,57)$$

► ***The effect of force*** F_z materializes in a shear stress for which:

$$\tau_{z1} = \left[1{,}7 \cdot d_{eb}^{\,2} \cdot \sin^2 \varphi^* \Big/ \left(d_{eb}^{\,4} - d_{ib}^{\,4} \right) \right] \cdot F_z , \qquad (5.\,58)$$

5. 6. Conclusions and perspectives

The content of this chapter addressed the issue of stress states in the structure of symmetrical flat lugs, as well as cylindrical trunnions, mounted along the radius of the cylindrical

structure of the anchored or erected equipment. At the same time, adequate relations for calculating the stresses developed in the welding cords are exposed, along the contact surface of the lug with the body of the equipment, respectively on the circumference when fixing the cylindrical trunnions.

The development of the study (numerical and / or experimental) for asymmetrical flat lugs is also suggested **[1, 40],** statically and / or dynamically loaded. The same goes for the trunnions, welded like the lugs, by means of reinforcement plates. In the sense of the above, it is also necessary to develop the calculations regarding the stress in the body of the equipment in the area where the lugs and trunnions are welded. The simplifying assumptions used in the calculations presented above can be accepted **[27, 41, 42].** Another idea is to study the stresses on the supports of the transported equipment, where the stability of the shape and the possible stiffening must be analyzed, with the appropriate influences in the anchoring systems **[2, 46, 47].**

CHAPTER 6

THEORETICAL AND EXPERIMENTAL STUDIES REGARDING CONSTRUCTIONS WITH LUGS AND TRUNNIONS FOR ANCHORING / LIFTING LOADS

6. 1. Introduction

As can be easily noticed, in the previous chapters, considering the operation of transporting industrial technological equipment, the aspects that can lead, in difficult situations, to special demands in the anchoring elements were highlighted: lugs, trunnions, as well as the related flexible elements (cables, chains, etc.).

6. 2. Description of the experimental stand

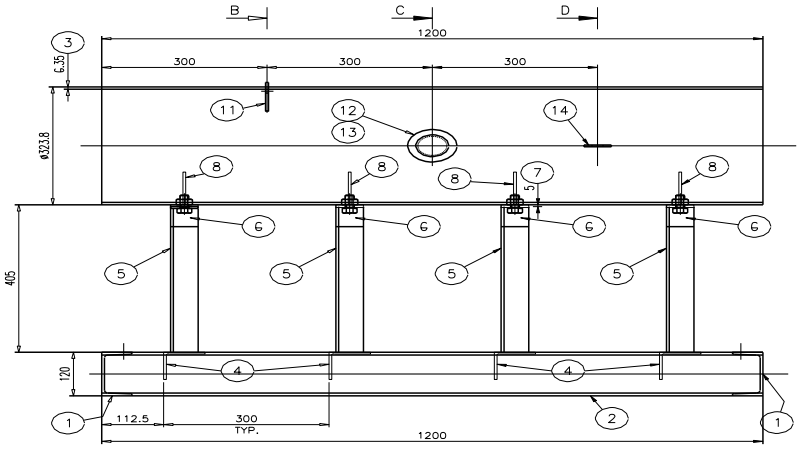

a)

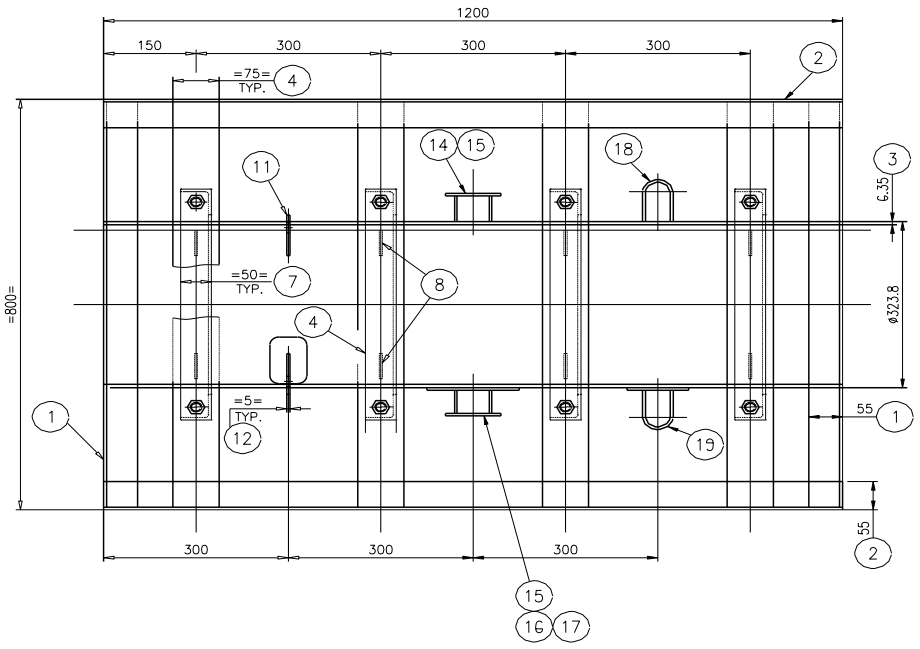

b)

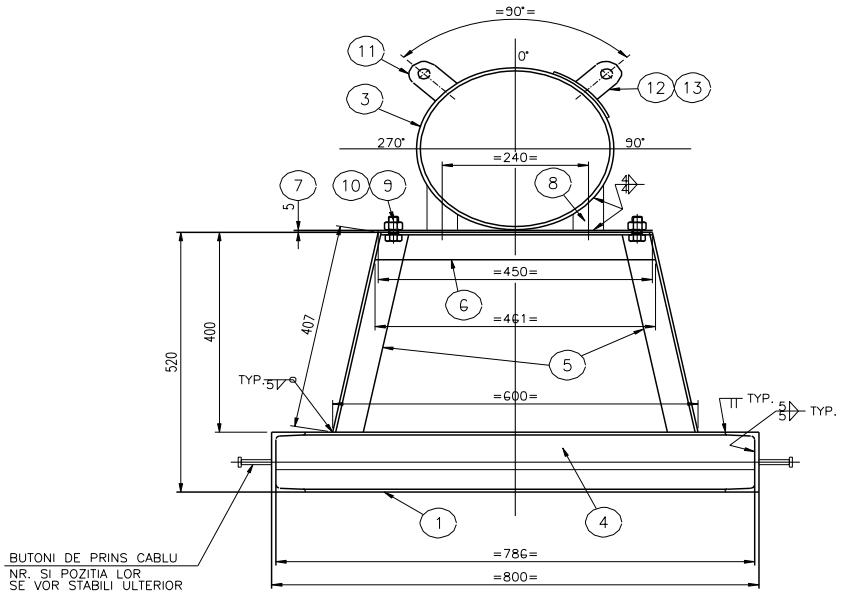

c)

Fig. 6. 1. Experimental stand (project)

a – side view; b – top view; c – side view

1, 2 – UPN 120 profiles: 3 – pipe; 4, 5, 6 – pressed profiles; 7 – plate; 8 - rib; 9 – screw; 10 – nut; 11, 12 – lug for anchoring; 13 – reinforcing plate; 14 – pipe; 15 – disc; 16 – pipe; 17 – reinforcing plate; 18, 19 – bar; 20 – reinforcing plate.

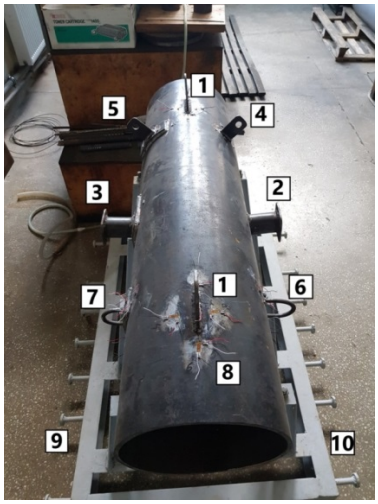

Fig. 6. 3. Experimental model - components

1- lifting ear, longitudinally placed (along the cylinder generator, without stiffening plate); 2 – trunnion for lifting / anchoring (without stiffening plate); 3 trunnion for lifting / anchoring (with stiffening plate); 4 – lug for lifting the cylinder in transverse plane, without stiffening plate; 5 – lug for lifting the cylinder in transverse plane, with stiffening plate; 6 – anchoring handle; 7 - anchoring handle with stiffening plate; 8 – tensometric transducers placed around a longitudinal placed lug; 9 – support frame; 10 – buttons used to fasten the lifting cables to the assembly support frame – experimental cylinder

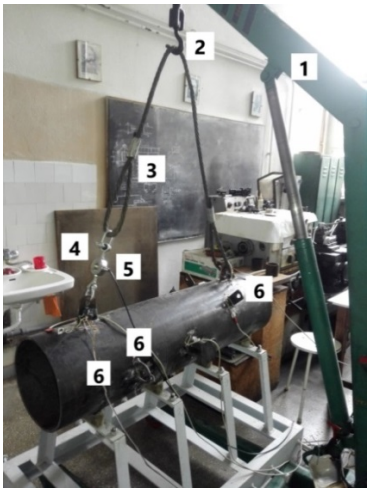

Fig. 6. 5. Experimental model positioned for lifting - Overview

1 - lifting crane (laboratory); 2 - lifting hook; 3 - cable used to lift the experimental model; 4 – shackle; 5 – force transducer; 6 – electrical cables connecting strain gauges to the apparatus for measuring specific linear deformations (strain gauge).

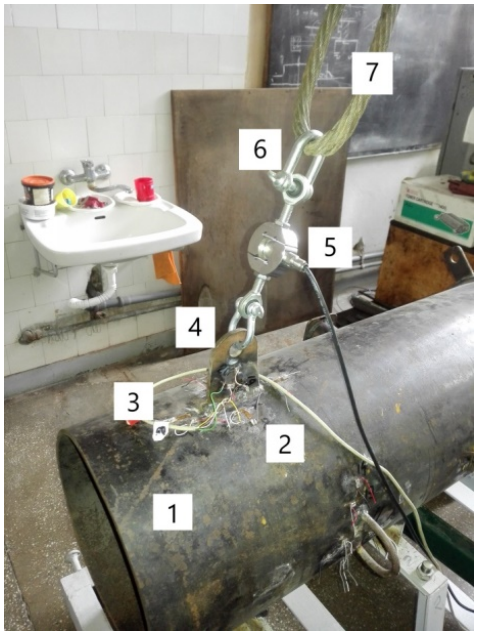

Fig. 6. 6. View from the grip area of an ear on the cylindrical body
1 – cylinder; 2 – strain gauges; 3 – electric circuit; 4 – lug for anchoring; 5 – force transducer; 6 – schackle; 7 - cable

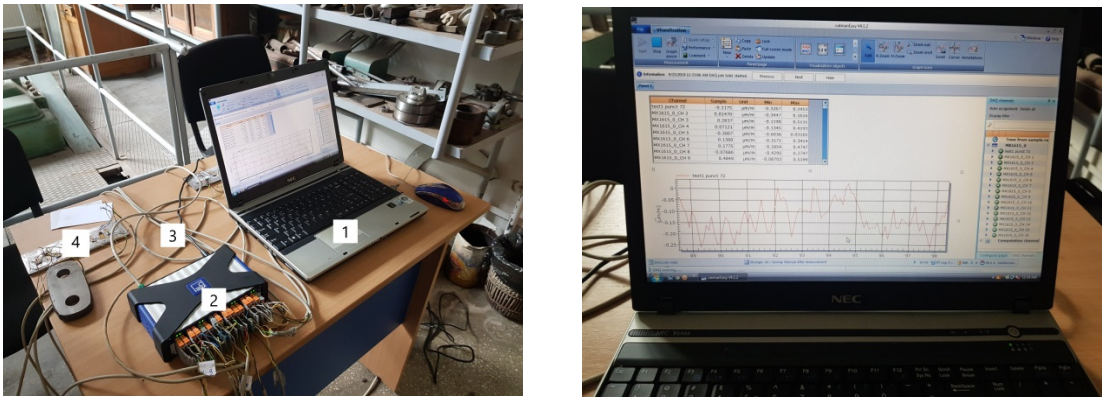

a) **b)**

Fig. 6. 8. Partial view with the equipment for recording the experimental values of the specific linear deformations (connection system type Quantum MX 1615, processing software type Cadman easy)
a – general view: b – laptop
1 – laptop; 2 – connection system; 3 – cablesi; 4 – strain gauges compensation plate

The experimental model, designed for experiments, consists essentially of a cylindrical body on which are welded lugs with and without reinforcing plates, along the generator and transversely to the cylindrical body, trunnions with or without reinforcing plates, hooks with or without reinforcing plates.

Note: Both the lugs and the trunnions are located on the model cylinder at distances greater than the half-wavelength:

$$l_s = 2,5 \cdot \sqrt{R \cdot \delta} = 2,5 \cdot \sqrt{158,725 \cdot 6,35} = 74,53\,mm\ ,$$

considering the geometry of the cylindrical body, designed (fig. 6. 1a).

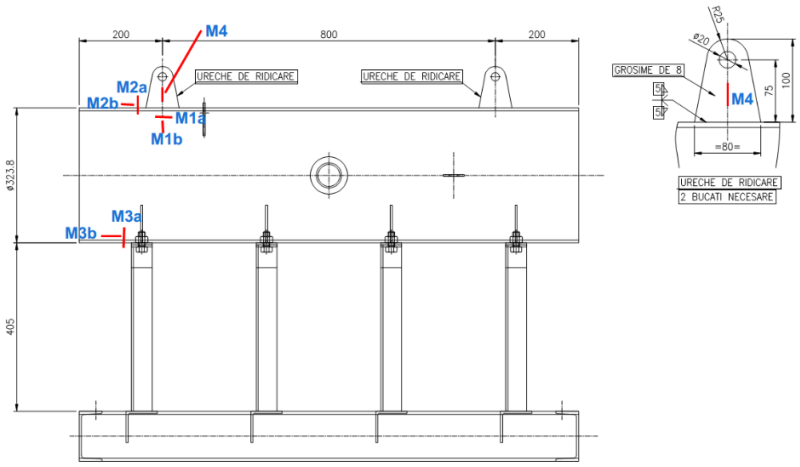

a)

b)

Fig. 6. 9. Positioning strain gauges around a flat lug
a – sketch (side view of the experimental model and lug geometry); b – top view of the strain gauges (electroresistive) positions, with 10 mm base.

6. 3. Flat lugs for anchoring / lifting [1, 2]

6. 3. 1. Experimental research

6. 3. 1. 1. Plane state of specific linear deformations

The experimental results were made on the device in figure 6.9, in which the horizontal cylinder has an outer diameter of 323.8 mm and a thickness of 6.35 mm. The thickness of the

lifting lug is 8 mm. The lifting force was obtained with the help of the laboratory crane and varied between 0 and 2,000 N.

The loading-unloading process took about 11 minutes. Experimental results were obtained continuously, but were noted (kept) for intervals of 200 N of the lifting force. The measurements were performed both during the loading operation and during the unloading operation.

The values of the specific linear deformations were noted at the same time from all strain gauges, being presented in table 6. 1.

Using the data presented in Table 6. 1, time dependencies of the specific linear deformations were drawn (Figures 6. 11 - 6. 14).

Analyzing the graphs of specific linear deformations, the following conclusions can be drawn:

a) the maximum specific linear deformations appear next to the marks M 3a and M 3b and have the values 128,58 $\mu m/m$, respectively 281,38 μ *m/m;*

b) the maximum specific linear deformations occur in the longitudinal direction of the cylinder, which is the main bending direction produced by the lifting forces;

c) the maximum specific linear deformations are located near the cylinder support, at which point the stresses intensify;

d) during the unloading process, at all measuring points, approximately the same values of the specific deformations were obtained (being compared with the same measuring points, but during the loading process);

e) at the end of the unloading process, when the lifting forces become zero, the deformations also remain zero, which proves that the experiment was performed in the elastic domain and at the end there were no residual deformations.

6. 3. 1. 2. Plane state of stress

Next, based on the specific linear deformations acquired and the generalized law of ***R. Hooke*** **[5, 6]** for the plane state of stresses, the following values were calculated (rounding the values to the third decimal - table 6. 2):

Based on the values of the tensions presented in table 6. 2, graphs of the time functions of the tensions were drawn (see figures 6. 15 - 6. 18).

A comparison between the experimental and theoretical results of the maximum stresses and for a lifting force equal to 1000 N, is presented in table 6. 3.

Tabel 6. 3. Experimental and theoretical results

Experimental and theoretical tensions	**M 2a - σ_{2a}**	**M 2b -- σ_{2b}**	**M 3a -- σ_{3a}**	**M 3b -- σ_{3b}**
Experimental results [MPa]	5,31	14,59	22,38	34,36
Theoretical results [MPa]	4,92	14,55	22,30	33,32
Relative error [%]	7 %	0,27 %	0,36 %	3 %

Conclusions

The above are the experimental results obtained by tensometric measurements for the anchoring lugs provided on the tested cylinder. The lifting lugs are 8 mm thick, while the cylinder thickness is 6.35 mm. It is found that the maximum stresses are transferred to the shell, in the junction area and near the support at the bottom.

The experimental results were very close in value to the theoretical ones, the maximum error being less than 7%. In fact, this maximum error occurs at low tension values, where it is well known that strain gauges do not allow high accuracy. For the other points, the maximum error does not exceed 3%.

6. 3. 2. Numerical analysis

The cylindrical shell analyzed below has the geometry shown in Figures 6.1a and 6. 9.

The material used for each component of the experimental device (S 235 JR) has the following physical - mechanical characteristics:

- Conventional yield stress : $R_e = 235\,MPa$;
- Tensile strength : $R_m = 360MPa$;
- Allowable stress: $\sigma_a = 205MPa$.

The specified experimental model was analyzed for two loading cases:

- **a)** When the vertical force (1,000 N) was applied directly to each lifting lug and the cylindrical ferrule remained fixed in a laboratory stand;
- **b)** During the lifting process, when the cylindrical shell is supported by the anchoring lugs and the vertical force in each of the studied lugs reaches the value of 1000 N.
- For each of the two cases of loading the cylindrical shell, different thicknesses were used for the lifting lugs, from 1 mm to 6 mm (the thickness of the cylindrical ferrule being 6.35 mm). The analyzed model is presented in figure 6. 19 (calculation program: COSMOS / M).

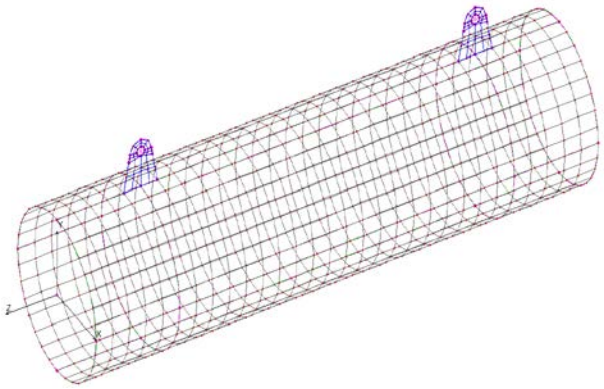

Fig. 6. 19. Numerical calculation model

6. 3. 2. 1. Results obtained

For the first loading case:

Analyzing the stress distributions, for various thicknesses of the lifting lugs, it can be seen that the maximum tension appears in the upper part of the ear 1 mm thick, where the vertical force is located, having the value of 123 MPa.

As the thickness of the lugs approaches that of the cylindrical shell, the maximum level of stress values moves from the top of the lifting ears to the cylinder in the area where they are welded. Starting with the 4 mm thickness of the ears, the maximum values of the tensions are approximately the same.

For the second loading case:

Analyzing the above tensions distribution, it can be seen that in both loading cases, the results are approximately the same, the most conservative case being the second, when the lifting lugs and the cylindrical shell are suspended in cables. It can also be seen that when the thickness of the lifting lugs is approximately equal to that of the cylindrical shell, the state of tension in the cylindrical shell - lifting lugs does not change.

6. 3. 2. 2. Conclusions

The maximum tensions obtained for the two load cases are shown below in Table 6. 4.

Analyzing the values of the maximum stresses presented above, it can be seen that in both loading cases, for lug thicknesses between 1 mm and 4 mm, the values are close. For thicknesses of lifting lugs close in value to the thickness of the cylindrical shell, larger differences can be observed between the two cases. The maximum stresses in case **b)** (which represent the actual situation during the lifting process) are lower, each time, than the maximum stresses obtained in the laboratory.

Table 6. 4. Maximum tensions obtained by FEA

Lifting lugs thickness [mm]	**Maximum tensions – Load case a) [MPa]**	**Maximum tensions – Load case b) [MPa]**	**Differences between the two loading cases [%]**
1	122,9	115,8	5,7
2	61,4	58,3	5,0
3	40,9	39,1	4,4
4	30,7	29,4	4,2
5	29,0	23,6	18,6
6	29,0	19,7	32,0

6. 4. Cylindrical trunnions for anchoring / lifting [3, 4]

6. 4. 1. Experimental research

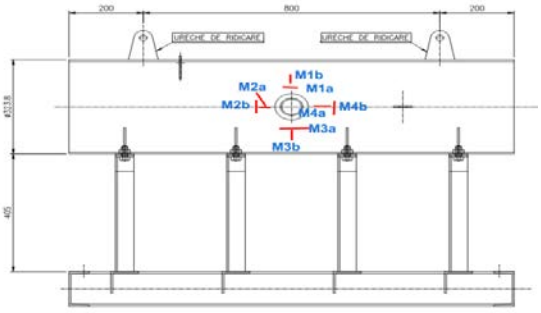

a)

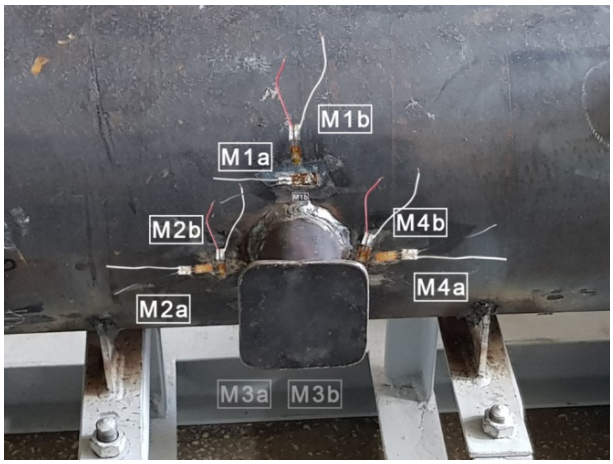

b)

c)

Fig. 6. 32. The experimental device with cylindrical trunnions

a – sketch with the location of the strain gauges; b – location of strain gauges in the case of the trunnion without reinforcing plate; c – placement of strain gauges (with 10 mm base) around the trunnion with reinforcing plate.

A total of 16 strain gauges were used, 8 for direct welding between the trunnion and the cylinder, and the other 8 for the junction with the reinforcing plate.

The experimental results were made on the device in figure 6. 32, in which the horizontal cylinder has an outer diameter of 324.8 mm and a thickness of 6.35 mm, and the lifting buttons are made of pipe with an outer diameter of 60.3 mm. and a thickness of 3.91 mm. The reinforcing plate is 5 mm thick.

6. 4. 1. 1. The plane state of specific linear deformations

The values of the specific linear deformations acquired for the strain gauges during the lifting process, for the **horizontally positioned cylinder**, are presented in tables 6. 5 and 6. 6. Table 6. 5 shows the values of the specific linear deformations acquired around the trunnion welded directly to the cylinder, and table 6. 6, the values acquired from the transducers positioned around the reinforcing plate.

The values of the specific linear deformations acquired by the srain gauges during the lifting process, for the **vertically positioned cylinder** are presented in tables 6. 7 and 6. 8. Table 6. 7 shows the values of the specific linear deformations acquired around the trunnion welded directly to the cylinder, and Table 6. 8, the corresponding values acquired from the transducers positioned around the reinforcing plate.

With the data presented in tables 6. 5 - 6. 6 time dependencies of the specific linear deformations were drawn: **a)** figures 6. 34 - 6. 37 for the trunnions welded directly to the horizontal cylinder; **b)** Figures 6. 38 - 6. 41 for trunnions welded on the horizontal cylinder togeteher with a reinforcing plate.

Analyzing the graphs of the specific linear deformations, the following conclusions can be drawn:

a) the maximum specific linear deformations, for the trunnions welded directly to the cylinder, appear next to the transducers M 1a and M 3a (positioned in the longitudinal direction) and have the values of approx 122 $\mu m/m$;

b) the maximum specific linear deformations, for the trunnions welded by a reinforcement plate on the cylinder, also appear next to the transducers M 1a and M 3a (positioned in the longitudinal direction) and have the values of approx 85 $\mu m/m$;

c) the use of the reinforcing plate decreased the values of the maximum specific linear deformations by approximately 35%;

d) during the unloading process approximately the same values of the specific linear deformations were obtained as those measured during lifting, which demonstrates that the experiment was performed in the elastic domain and at its end there were no residual deformations.

Next, with the data presented in tables 6. 7 and 6. 8, time dependencies of the specific linear deformations were drawn: **a)** figures 6. 42 - 6. 45 for welded trunnions directly on the cylindrical body and **b)** figures 6. 46 - 6. 49 for trunnions welded by a reinforcing plate on the cylindrical body.

Analyzing the graphs of the specific linear deformations, the following conclusions can be drawn:

a) the maximum specific linear deformations, for the trunnions welded directly on the cylinder body, appear next to the transducers M 1a and M 3a (positioned in the longitudinal direction) and have values of approx 120 $\mu m/m$;

b) the maximum specific linear deformations, for the trunnions welded by a reinforcing / stiffening plate on the cylinder, also appear next to the transducers M 1a and M 3a (positioned in the longitudinal direction) and have the values of approx 62 *μm/m;*

c) the use of the reinforcing / stiffening plate decreased the values of the maximum specific linear deformations by approximately 50%;

d) during the unloading process approximately the same values of the specific linear deformations were obtained as those measured during lifting, which demonstrates that the experiment was performed in the elastic domain and at its end there were no residual deformations.

6. 4. 1. 2. Plane stress state

Next, based on the acquired specific linear deformations and the generalized law of ***R. Hooke*** for the plane state of stresses **[5, 6],** the following stresses were calculated :

a) longitudinal and circumferential stresses around the welded trunnions directly on the horizontal cylinder - table 6. 9;

b) longitudinal and circumferential stresses around the trunnions welded to the horizontal cylinder by a reinforcing plate - table 6. 10;

c) longitudinal and circumferential stresses around the welded trunnions directly on the vertical cylinder - table 6. 11;

d) longitudinal and circumferential stresses around the trunnions welded to the vertical cylinder through a reinforcing plate table 6. 12.

Based on the values presented in tables 6. 9 - 6. 12 the following time functions (of tensions) were drawn:

a) longitudinal and circumferential stresses around the welded trunnions directly on the horizontal cylinder (fig. 6. 50 - 6. 53);

b) the longitudinal and circumferential tensions around the trunnions welded to the horizontal cylinder through a reinforcing plate (fig. 6. 54 - 6. 57);

c) longitudinal and circumferential stresses around the welded buttons directly on the vertical cylinder (fig. 6. 58 - 6. 61);

d) longitudinal and circumferential stresses around the welded trunnions on the vertical cylinder through a reinforcing plate (fig. 6. 62 – 6. 65).

Analyzing the time functions of the tensions (fig. 6. 50 - 6. 65) the following conclusions can be drawn:

a) the maximum normal stresses that appear around the lifting trunnions, if they are **welded directly on the horizontal cylinder** are approximately 27 MPa (fig. 6. 50, 6. 52) and have symmetric values at points M 1 and M 3, as expected;

b) the maximum normal stresses at points M 2 and M 4, for the trunnions **welded directly to the horizontal cylinder** are also symmetrical, but have lower values of about 3 MPa;

c) the maximum normal stresses that appear around the lifting trunnions, if they are **welded to the horizontal cylinder through a reinforcing plate** are about 19 MPa (fig. 6. 54, 6.

56) and have symmetric values at points M 1 and M 3, as expected; the presence of the stiffening plate reduces the intensity of the maximum stresses by approximately 33%;

d) the maximum normal stresses at points M 2 and M 4, for the trunnions **welded to the horizontal cylinder by a reinforcing plate** are also symmetrical, but have lower values, of about 3 MPa;

e) the maximum normal stresses that appear around the lifting trunnion, if they are **welded directly on the vertical cylinder** are about 26 MPa (fig. 6. 58, 6. 60) and have symmetric values at points M 1 and M 3, as expected; compared to the horizontal cylinder, the direction in which they are maximum changes;

f) the maximum normal stresses at points M 2 and M 4, for the trunnions **welded directly to the vertical cylinder** are also symmetrical, but have lower values of about 3.5 MPa;

g) the maximum normal stresses that occur around the lifting trunnions, if they are **welded to the vertical cylinder through a reinforcing plate** are about 18 MPa (fig. 6. 62, 6. 64) and have symmetric values at points M 1 and M 3, as expected; the presence of the reinforcing plate reduces the values of the maximum stresses by approximately 38%;

h) the maximum normal stresses at points M 2 and M 4, for the trunnions **welded to the vertical cylinder by a reinforcing plate** are in turn symmetrical, but have lower values of about 3.5 MPa.

A synthesis of the experimental results (for the values of the maximum normal stresses) is presented in table 6. 13, where a comparison between the experimental and the theoretical values is made, resulting from an analysis with the finite element method.

The maximum errors obtained from the measurements show that the experiment was performed with very good accuracy, the difference between the theoretical results (obtained by the finite element method) and the experimental ones being less than 5%.

Table 6. 13. Theoretical and experimental results for tensions [MPa]

Theoretical and experimental results	**Maximum normal tensions a)**	**Maximum normal tensions b)**	**Maximum normal tensions c)**	**Maximum normal tensions d)**
Experimental results	27.07	19.01	28.79	17.74
Theoretical results *)	27,74	19,75	27,33	16,97
Relative error	2.5 %	3.8 ^%	5.0 %	4.3 ^%

***)** Results obtained by the finite element method, with COSMOS M program (paragraph 6. 4. 2)

a – **horizontal cylinder** – trunnions welded directly; **b** – **horizontal cylinder** - trunnions welded on a reinforcing plate; **c** – **vertical cylinder** - trunnions welded directly; **d** – **vertical cylinder** - trunnions welded on a reinforcing plate (the horizontal and vertical position of the cylinder is used for testing).

6. 4. 1. 3. Conclusions

IThe above shows the experimental results, obtained by tensometric measurements around lifting trunnions welded on a cylinder, directly on its surface or by means of a reinforcing plate. The experiment was performed for two extreme positions of the lifting process: the horizontal and the vertical.

The experimental results were very close to the theoretical ones, the maximum error being 5%.

6. 4. 2. Numerical analysis

6. 4. 2. 1. General aspects

The analyzed cylinder and the cylindrical lifting / anchoring trunnions have the geometry shown in figure 6. 66. As can be seen, one trunnion is welded directly to the cylindrical shell and the other is welded by means of a reinforcing plate, which is positioned between the button and the outer surface of the cylinder.

For the calculation model made by the finite element method (fig. 6. 67) several load cases were made :

I) fixing (clamping) the support cylinder and stressing with a vertical force of 1,000 N, for each trunnion tested;

II) lifting the cylinder by the trunnions and stressing it with its weight, during the lifting process, when it reaches an inclination of 45^{o} from the horizontal;

III) stressing the cylinder with its own weight, when it has reached the vertical position.

In the load cases a) and c) two possibilities of fastening the trunnions on the cylindrical shell were considered: by direct welding on the cylinder and by welding on an intermediate reinforcing plate.

Also, for each load case, various thicknesses of the lifting trunnions were simulated, starting from 1.65 mm, up to 8.74 mm (the thickness of the cylinder being 6.35 mm).

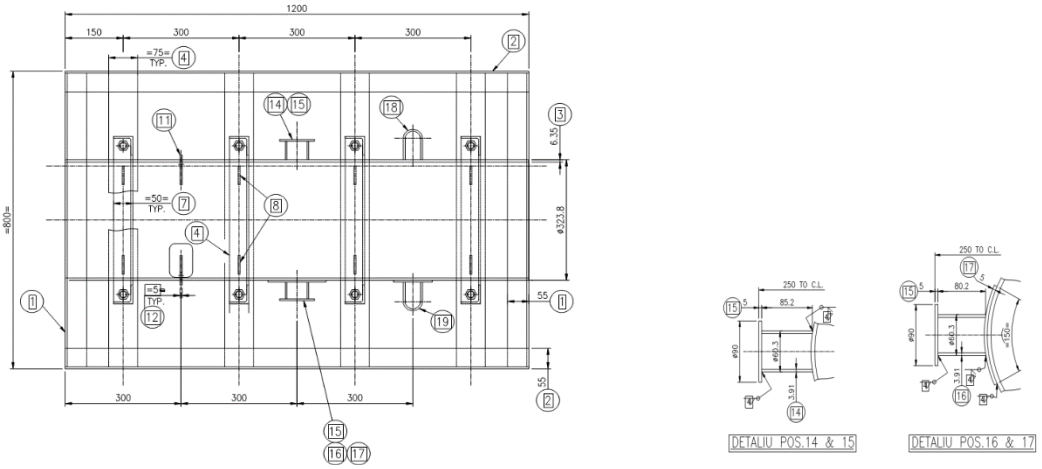

a) **b)**

Fig. 6. 66. Cylindrical shell overview

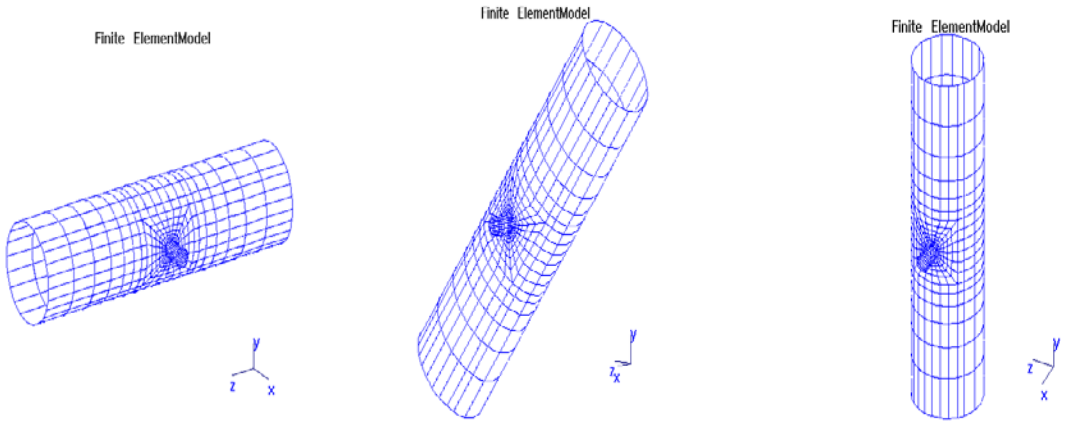

a) case a) loading b) case b) loading c) case c) loading

Fig. 6. 67. Calculation model with the finite element method

6. 4. 2. 2. Results obtained

For case I) loading, when the cylinder is located in a horizontal position and is fixed to the support, the tension distributions, for various thicknesses of the lifting buttons, are shown in figures 6. 68 - 6. 73.

Analyzing the tension distributions for various thicknesses of the lifting trunnions, the following conclusions can be drawn:

a) for the smallest thickness of the lifting trunnions (1.65 mm), the maximum tension has the value of 165 MPa and appears in the trunnions, at the junction between them and the cylinder; the same situation appears for the thickness of the trunnions of 2.77 mm, the only difference being that the value of the maximum tension decreases up to 120 MPa;

b) as the thickness of the trunnions increases and approaches that of the cylinder, the maximum level of stress values decreases and they discharge into the cylinder; the cylinder begins to participate more "**actively**" in the resistance of the whole structure; for a trunnion thickness of 3.91 mm, the maximum stresses also appear at the base of the trunnions and have the value of 77 MPa, and for a trunnion thickness of 5.54 mm the maximum stresses appear both in the cylinder and trunnions, having the value of 58 MPa;

c) the lowest level of stress values occurs when the thickness of the buttons is equal to that of the cylinder; the maximum stresses also appear in the junction area, but are distributed more per cylinder, having the value of 47.3 MPa;

d) for a button thickness greater than that of the cylinder (8.74 mm compared to 6.35 mm), the level of maximum stress values begins to increase and reaches the value of approximately 50 MPa.

Noting the above conclusions it can be observed that the most favorable situation is represented by the case when the anchoring trunnions have the same thickness as that of the cylinder.

In the second loading case, **II),** when the cylinder is tilted to 45^{o} (to the horizontal or vertical) and it is fixed to the support, the tension distributions, for various thicknesses of the anchoring / lifting trunnions, are shown in figures 6. 74 - 6. 79.

Observing the tension distributions for various thicknesses of the anchor / lift buttons, the following conclusions can be drawn:

a) for the smallest thickness of the lifting trunnions (1.65 mm) the maximum tension has the value of 140 MPa and appears in the trunnions, at the junction between them and the cylinder; the same situation occurs for the thickness of the trunnions of 2.77 mm, the only difference being that the value of the maximum tension decreases up to 95 MPa;

b) as the thickness of the trunnions increases and approaches that of the cylinder, the maximum level of tension decreases; these tensions are also discharged into the cylinder, which begins to participate more "actively" in the strength of the entire structure; for a trunnion thickness of 3.91 mm, the maximum stresses also appear at the base of the trunnions and have the value of 66 MPa, and for a trunnion thickness of 5.54 mm the maximum stresses appear in the cylinder, with the value of 42.33 MPa;

c) the lowest level of stress values occurs when the thickness of the trunnions is equal to that of the cylinder; the maximum stresses also appear in the junction area, but they are distributed more on the cylinder and have the value of 39.45 MPa;

d) for a trunnion thickness greater than that of the cylinder (8.74 mm compared to 6.35 mm), the level of maximum stress values starts to increase and reaches the value of approximately 41.71 MPa.

Analyzing the above conclusions it can be seen that the most favorable situation occurs if the anchor trunnions have the same thickness as the cylinder.

In the third case of loading, **III),** when the cylinder is in a vertical position, under its own weight (the tension distributions, for various thicknesses of the anchoring trunnions, are shown in figures 6.80 - 6. 85).

From the analysis of the above figures for the tension distributions in case of various thicknesses of the anchoring trunnions, the following conclusions can be drawn:

a) for the smallest thickness of the anchoring trunnions (1.65 mm) the maximum tension has the value of 141 MPa and appears in the trunnions, at the junction between them and the cylinder; the same situation appears for the thickness of the trunnions of 2.77 mm, the only difference being that the value of the maximum tension decreases up to 73.72 MPa;

b) as the thickness of the trunnions increases and approaches that of the cylinder, the maximum level of tension decreases and they are discharged into the cylinder, which begins to participate more "**intensely**" in the strength of the entire structure; for a trunnion thickness of 3.91 mm, the maximum stresses also appear at the base of the trunnions and have the value of 50.89 MPa, and for a trunnion thickness of 5.54 mm the maximum stresses appear both in the cylinder and trunnions, having the value of 31.8 MPa;

c) the lowest level of stress values occurs when the thickness of the trunnions is equal to that of the cylinder; maximum stresses also occur in the junction area, but are distributed more per cylinder, with a value of 30.64 MPa;

d) for a thicker trunnion than the cylinder (8.74 mm vs. 6.35 mm), the maximum stress level begins to rise and reaches approximately 31.7 MPa.

Analyzing the above conclusions it can be seen that the most favorable situation occurs if the anchor trunnions have the same thickness as the cylinder.

6. 4. 2. 2. 2. Trunnions welded to the cylinder by means of a reinforcing plate

Next, the same load cases were analyzed, for the situation in which, between the anchoring trunnions and the cylinder, there is a reinforcing plate (stiffening) with a thickness of 5 mm.

For loading case I), when the cylinder is located in a horizontal position and is fixed to the support, the tension distributions, for various thicknesses of the lifting trunnions, are shown in figures 6. 86 - 6. 91.

Looking at the figures with the tension distributions for various thicknesses of the lifting trunnions, the following conclusions can be drawn:

a) for the smallest thickness of the anchoring trunnions (1.65 mm) the maximum value of the tension is 54.44 MPa which appears in the trunnions, at the junction between them and the stiffening plate; the same situation appears for the thickness of the trunnions of 2.77 mm, the only difference being that the value of the maximum tension decreases up to 45.68 MPa;

b) as the thickness of the trunnions increases and approaches that of the stiffening plate, the maximum level of stresses decreases and they are discharged into the plate as well, beginning to take over some of the maximum stresses; for a trunnion thickness of 3.91 mm, the maximum stresses also appear at the base of the trunnions and have the value of 36.42 MPa, and for a trunnion thickness of 5.54 mm the maximum stresses appear both in the plate and trunnions, with the value of 28.74 MPa;

c) as the thickness of the trunnions increases, the values of the maximum stresses decrease, so that, for a thickness of the trunnions of 6.25 mm, the maximum stresses are 25.22 MPa, and for a thickness of 8.74 mm the maximum stresses reach the value of 17.84 MPa;

d) the presence of the stiffening plate reduces the level of maximum stresses at the junction and causes the level of maximum stresses to decrease even when the anchor trunnions have a greater thickness than that of the cylinder.

In the second loading case, **II),** when the cylinder is tilted to 45^{o} (to the horizontal or vertical) and is fixed to the support, the tension distributions, for various thicknesses of the anchor trunnions, are shown in Figures 6. 92 - 6. 97.

The following conclusions can be drawn from the study of the stress distributions for various thicknesses of the anchoring trunnions:

a) for the smallest thickness of the anchoring trunnions (1.65 mm) the maximum tension of 52.44 MPa appears in the trunnions, at the junction between them and the stiffening plate; the same situation appears for the thickness of the trunnions of 2.77 mm, the only difference being that the value of the maximum tension decreases up to 41.16 MPa;

b) as the thickness of the trunnions increases and approaches that of the stiffening plate, the maximum level of stresses decreases and they also discharge into the stiffening plate, which begins to take over some of the maximum stresses; for a trunnion thickness of 3.91 mm, the maximum stresses also appear at the base of the trunnions and have the value of 33.66 MPa, and for a trunnion thickness of 5.54 mm the maximum stresses appear both in the plate and trunnions, having the value of 25.75 MPa;

c) as the thickness of the trunnions increases, the values of the maximum stresses decrease, so, for a thickness of the trunnions of 6.35 mm, the maximum stresses are 22.68 MPa, and for a thickness of 8.74 mm the maximum stresses reach the value of 16.03 MPa;

d) the presence of the stiffening plate reduces the level of maximum stresses at the junction and causes the level of maximum stresses to decrease even when the anchor trunnions have a thickness greater than that of the cylinder.

In the third loading case, **III),** when the cylinder is in a vertical position, under its own weight, the tension distributions, for various thicknesses of the anchoring trunnions, are shown in figures 6. 98 - 6. 103.

The following conclusions can be drawn based on the tension distributions for various thicknesses of the anchor trunnions:

a) for the smallest thickness of the anchoring trunnions (1.65 mm) the maximum tension of 46.53 MPa appears in the trunnions, at the junction between them and the stiffening plate; the same situation appears for the thickness of the trunnions of 2.77 mm, the only difference being that the value of the maximum tension decreases up to 36 MPa;

b) as the thickness of the trunnions increases and approaches that of the stiffening plate, the maximum level of stresses decreases and they are discharged into the plate, which begins to take over some of the maximum stresses; for a trunnion thickness of 3.91 mm, the maximum stresses also appear at the base of the trunnions and have the value of 28.15 MPa, and for a trunnion thickness of 5.54 mm the maximum stresses appear both in the plate and trunnions with the value of 22.14 MPa;

c) as the thickness of the trunnions increases, the values of the maximum stresses decrease, so, for a thickness of the trunnion of 6.35 mm, the maximum stresses are 19.38 MPa, and for a thickness of 8.74 mm the maximum stresses reach the value of 13.67 MPa;

d) the presence of the stiffening plate reduces the level of maximum stresses at the junction and causes the level of maximum stresses to decrease even when the anchor buttons have a thickness greater than that of the cylinder.

In all the loading cases, the presence of the stiffening plate reduces the level of maximum stresses at the junction and is a more favorable situation, recommended for anchoring technological equipment during their transportation.

6. 4. 3. Global conclusions

The above shows the stresses that occur at a junction between a cylindrical technological equipment and its anchoring trunnions (on the transport platforms) or lifting (in the handling phases), in specific positions:

I) in a horizontal position;

II) in an inclined position at 45^{o} to the horizontal or vertical;

III) in vertical position (under the effect of own weight - handling phases).

All three cases presented above were analyzed in two common cases:

a) when the anchor trunnions have been welded directly to the outer surface of the cylinder;

b) when a stiffening plate has been mounted between the anchoring trunnions and the cylindrical body (in this case circular in shape; a square plate is present on the experimental cylinder).

The results obtained in all the cases specified above were analyzed for various thicknesses of the cylindrical trunnions, summarized in table 6. 14.

The values of the maximum stresses presented in table 6. 13 allow the following observations:

a) the presence of the stiffening plate is more favorable, as it reduces the level of maximum stresses by almost half;

b) in the absence of the stiffening plate, it should be noted that the thickness of the lifting / anchoring trunnions should not be increased above that of the cylinder, as the maximum stresses begin to increase.

Table 6. 14. Maximum stresses established by the finite element method

How the trunnion is fixed on the cylindrical body	Thickness of anchor trunnions [mm]	Maximum stress – case I [MPa]	Maximum stress – case II [MPa]	Maximum stress – case III [MPa]	Remarks
Welded directly on the cylindrical body	**1,65**	162,3	139,9	141,8	there is an increase in stress values when the thickness of the trunnions exceeds the thickness of the cylinder
	2,77	118,9	94,62	73,72	
	3,91	77,21	65,65	58,84	
	5,54	57,86	42,33	31,36	
	6,35	47,27	39,45	30,64	
	8,74	49,97	41,71	31,78	
Welded by means of a stiffening plate	**1,65**	57,44	52,44	46,53	the intensity of the tensions also decreases when the thickness of the buttons becomes greater than that of the cylinder
	2,77	45,68	41,16	35,98	
	3,91	36,42	32,66	28,15	
	5,54	28,74	25,75	22,14	
	6,35	25,32	22,68	19,38	
	8,74	17,84	16,83	13,67	

CHAPTER 7

CONCLUSIONS. CONTRIBUTIONS. PERSPECTIVES

7. 1. Conclusions

Since his appearance of the man on Earth, in order to survive, he has sought ways to manipulate primary products (fruits, game) by force or alternative variants: stretcher, sleigh, cart (after the invention of the wheel), as a result of domestication of animals (horse, ball etc.). Subsequently, moving to the production of semi-industrial and industrial products, by discovering the steam engine or internal combustion, we proceeded to the realization of towing means (locomotives, ships, wheeled vehicles with tires or tracks) performing on both roads, railways, by water or air (including travel in the cosmos).

This paper addresses the possible transportation of oversized technological equipment, produced as a result of the realization of products from the chemical and petrochemical industry, the construction materials industry, the food industry, plastics, etc. The performance of the physico-chemical processes required the construction of larger and more complex equipment, which should work in conditions, with working parameters with high or low values (pressures, temperatures, chemically and / or mechanically aggressive environments), in technical / technological safety conditions. New manufacturing, transport and assembly technologies have been perfected or created (the existence of high capacity lifting and transporting machines). One of the very important operations in the manufacturing and commissioning stages is the transportation of large-scale technological equipment with appreciable masses. Such a complex operation is performed in difficult conditions in terms of road conditions and actions (generally unfavorable) of external loads (static or, especially, dynamic). The thesis draws attention to the need for the safe anchoring of the equipment of the kind mentioned on the road transport platforms, in this case, but not only.

7. 2. Contributions

a) For a start, the history of transporting technological products with adequate equipment is reviewed, relatively briefly. The advantages and disadvantages for each type of handling are highlighted, highlighting road, rail, water or air transport.

b) Through study of technical-scientific literature it is presented elements of calculation of the forces necessary for carrying out oversized and high mass transports, taking into account the characteristics of towing means, equipment, but also the effect of external loads and road conditions **(chapter 2 – personal contributions: bibliographic sources - pos. 44, 45, 46).** For example, the case of transport with the help of two remote platforms (frequently used for long-term technological equipment), when moving in a straight line or in curves was chosen.

c) Opinions from the literature on the analysis of the conditions for ensuring the stability of the longitudinal movement of towing vehicles (two- or three-axle trailers, wheeled or tracked tractors), as well as the case (chosen) of two distant platforms when climbing or when descending a slope, respectively transporting with semi-trailers, with or without neglecting the deformation of the suspensions and tires **(chapter 3 – personal contributions: bibliographic sources - pos. 20 … 23, 25).**

d) Study of the literature on the conditions necessary to ensure the transverse stability of the movement of wheeled or tracked vehicles, as well as of coupled platforms, loaded with oversized technological equipment **(chapter 4 – personal contributions: bibliographic source – pos. 7).**

e) The study, appreciated as detailed, from the profile literature, with reference to the presence of simple, welded flat lugs, and cylindrical trunnions, usually used for lifting or

anchoring mass loads (but also for cases with geometries with difficulty moving, possibly with changes in the route in question) **(chapter 5 – personal contributions: bibliographic sources – pos. 19, 20, 48)** . The industrial practice of direct welding of the erected / anchored shell or by means of intermediate stiffening plates is considered, with favorable effects for the state of tensions. Attention is drawn to the correlation of the overall geometry of the transported equipment and the transport platforms.

f) Experimental (electro-tensometric measurements) and theoretical (finite element method - FEA / MEF) research on flat lugs and cylindrical trunnions.

► Realization of an experimental stand consisting of a cylindrical body provided with a support in welded construction, with the possibility of detachment during testing. Flat lugs (with or without reinforcement plate) and cylindrical trunnions (with or without stiffening plate) were welded to the cylindrical body. – (**par. 6. 2**).

► Electro-tensometric measurements were performed with resistive transducers with a base of 10 mm. The collection of the experimental results and the processing were performed with a connection system type Quantum MX 1615, processing software type Cadman easy.

► For the experimental analysis of the flat lugs welded directly by the cylindrical container, the positioning of the electro-resistive transducers is illustrated in **figure 6. 9.**

- The values recorded for the specific linear deformations, both when lifting and when reducing the force developed by the laboratory crane, are given in **table 6. 1**, and their graphical representation is illustrated by **figures 5. 11 – 6. 14**. The maximum stress is found in the area of attachment of the container with the support (**transducers M3a, M3b – fig. 6.9a**). Regarding the positioning of the lugs, the measurements highlight the bending stress on the left edge of the left lug (**fig.6. 3 – pos. 1; fig. 6. 4, lifting system – fig. 6. 5 – fig. 6. 6 – fig. 6. 9**). The lifting was performed as noted in **figurile 6. 5 – 6. 7.**
- The values of the stresses in the flat state of stress, with the help of the deformations indicated in table 6. 1, are given in **table 6. 2**, respectively in **figurile 6. 15 – 6. 18**. The conclusions are identical to those mentioned above.

► **Figure 6. 32** offers positioning of electro-resistive transducers around cylindrical trunnions, without or with stiffening plate.

- The values recorded for the specific linear deformations are presented in **table 6. 5** – trunnion welded directly to the cylindrical body and **figures 6. 34 – 6.41**, respectively in **table 6. 6** – trunnion welded to the cylindrical body by means of a stiffening plate and **figures 6. 42 – 6. 49**.
- The flat state of stresses, calculated on the basis of the values of the deformations registered when the lifting force rises and falls, is given by means of the following tables and figures:

a) For the cylinder in a horizontal position and the trunnion welded directly to the cylinder **table 6. 9** contains the tension values, graphically in **figures 6. 50 – 6. 57**; the tension values for the case with the stiffening plate trunnion are given by **table 6. 10**, graphic illustrated in **figures 6. 54 – 6. 57**.

b) For the cylinder in the vertical position, the trunnion being welded directly to the cylinder **table 6. 11** contains the tension values, graphically in **figures 6. 58 – 6. 61**; the tension values for the case with the stiffening plate trunnion are given by **table 6. 12**, graphic illustrated in **figures 6. 62 – 6. 65.**

c). Appropriate conclusions for the deformation and stress states, useful for practical conditions, are drawn for both positions of the tested cylinder.

► **Numerical analysis,** using **finite element method**, for cylindrical trunnions welded directly to the cylindrical body or by means of a stiffening plate, was carried out for three positions: horizontal cylinder, inclined at 45^0 compared to the horizontal and the vertical. It is also mentioned that several thicknesses of the trunnion wall were considered (1, 65; 2,77; 3,91; 5,54; 6,35; 8,74 mm), keeping the thickness of the cylindrical body wall constant, of 6,35 mm. The intensity of the tension state, illustrated by the appropriate pictograms, for the mentioned cases will be specified as follows:

a) Trunnions welded directly to the cylindrical body of the vessel:

- horizontal position of the cylinder: fig. 6. 68 – 6. 73:
- inclined position at 45^0 compared to the horizontal: fig. 6.74 – 6. 79;
- vertical position of the cylinder: fig. 6. 80 – 6. 85.

b) Trunnions welded to the cylindrical body of the container by means of a stiffening plate:

- horizontal position of the cylinder: fig. 6. 86 – 6. 91:
- inclined position at 45^0 compared to the horizontal: fig. 6.92 – 6. 97;
- vertical position of the cylinder: fig. 6. 98 – 6. 103.

► From the study of the states of tension developed at the joint of the vessel body and the trunnions, it stands out:

a) the presence of the stiffening plate is more favorable, as it reduces the level of maximum stresses by almost half;

b) in the absence of the stiffening plate, it should be noted that the thickness of the lifting / anchoring trunnions should not be increased above that of the cylinder, as the maximum stresses begin to increase.

► **Bibliography positions 1 - 3** from **chapter 6** indicates useful personal contributions in solving the objectives proposed in the experimental part and numerical analysis of the structures with lugs and cylindrical trunnions for lifting / anchoring.

7. 3. Perspective

Further perspectives are proposed for further research:

a) the influence of more steep slopes, even with unevenness (inside the construction sites, for example) and various travel regimes;

b) analysis of joining the curves with variable speed, considering the characteristics of the surface of the route and the transversal inclination;

c) analysis of the variable influence of the effects of wind loads;

d) evaluation of entering and exiting of the transport platforms, respectively the trajectories on which the towing vehicles move, correlated with the geometry of the existing roads and necessary modifications / adaptation;

e) the influence of the special vibrating regime appeared on the uneven roads, especially inside the construction sites, both on the driver(s) and on the load;

f) the stability of the longitudinal movement of multi-axle vehicles;

g) correct evaluation of all loads that occur in the anchor points, for sizing or checking the geometry of the lugs, respectively the trunnions;

h) Further research on the intensity of stress states under different dynamic loads, based on a recorded statistical situation:

- in the structure of the welding seams at the base of the lugs;
- in the case of asymmetrical or double lugs:
- in case of fixing the lugs on the cylindrical body different from the normal position on the geometric axis:
- study the effects of dynamic loads by adopting an overload coefficient for equipment handling operations;
- for the existing structures on the foundations, the fatigue analysis of the ears for anchoring can be done, by considering the influence of wind or seismic loads.